Table S1. Summary of gene expression changes in *ess1* mutants

A

Experiment	# genes (>2-fold change)			
	(24°C)		(34°C)	
ess1^{H164R} *vs.* wild-type	up	down	up	down
	43	117	253	378
pGAL-H164R *vs.* pGAL-ESS1	uninduced		induced (+100 nm β-estradiol)	
	up	down	up	down
	233	409	285	75

B

ORF	gene name	rank order in *ess1* mutants	fold increase in *ess1* mutants	fold increase in *ssu72* mutants[a]	upstream snoRNA
YDR042C		1	42.3	12.1*	Snr47
YHR157W	*REC104*	2	34.0	11.2*	Snr71
YCRO15C		3	29.0	28.9	Snr33
YOR278W	*HEM4*	6	12.5	n.a.	Snr5
YGL098W	*USE1*	9	11.0	n.a.	Snr82
YCR014C	*POL4*	14	7.20	5.0	Snr33
YIL134W	*FLX1*	16	6.76	25.2	Snr68
YPR091C		17	6.53	11.4	Snr41
YKL006C	*SFT1*	19	6.06	n.a.	Snr87
YJL048C	*UBX6*	25	5.19	5.5*	Snr60
YDR472W	*TRS31*	29	4.66	5.7	Snr13
YOL034W	*SMC5*	36	4.39	4.1	Snr50
YLR105C	*SEN2*	51	3.51	10.0	Snr79

[a] Data from Ganem *et al*.,(2003) and (*) Nedea *et al*., (2003)
n.a. not available

Table S1C

Top 50 up-regulated genes *ess1-ts* vs. wild type

	Identifier	UniGene Symbol	ts vs. wt at 34°C	ts vs. wt 0-estradiol	Combinec	UniGene Name
1	YDR042C		42.32	32.12	36.87	Hypothetical ORF
2	YHR079C	SAE3	17.36	28.80	22.36	Protein involved in DNA repair...
3	YHR157W	REC104	34.04	14.26	22.03	meiosis-specific protein
4	YCR015C	NA	29.02	13.54	19.82	Hypothetical ORF
5	YCL007C	NA	6.02	17.34	10.22	NA
6	YOR278W	HEM4	12.47	8.10	10.05	uroporphyrinogen III synthase
7	YGL098W	USE1	10.95	7.99	9.36	Use1p is a SNARE / trafficking Golgi to ER
8	YMR107W	NA	4.63	17.51	9.01	Req. for survival at high temperature...
9	YBR119W	MUD1	6.88	8.33	7.57	U1 snRNP A protein
10	YOR237W	HES1	14.22	3.20	6.75	similar to human oxysterol binding protein
11	YKL037W	NA	5.25	7.96	6.46	Hypothetical ORF
12	YOL154W	ZPS1	9.33	3.93	6.05	Putative GPI-anchored protein…
13	YPL192C	PRM3	7.32	4.83	5.95	Pheromone-regulated, req. for karyogamy…
14	YJL048C	UBX6	5.19	6.62	5.86	Protein of unknown function…
15	YML058W	HUG1	11.16	2.86	5.65	Involved in Mec1p-mediated checkpoint…
16	YPR091C	NA	6.53	4.83	5.62	Hypothetical ORF
17	YIL024C	NA	5.91	5.31	5.60	Hypothetical ORF
18	YHR079C	SAE3	4.66	6.09	5.33	Involved DNA repair, meiotic recombination…
19	YML083C	NA	11.57	2.43	5.30	Hypothetical ORF
20	YLR202C	NA	4.84	5.60	5.21	Localized to the mitochondria
21	YKL006C	SFT1	6.06	4.44	5.19	v-SNARE
22	YJR158W	HXT16 /// H	2.97	8.71	5.09	hexose permease /// hexose transporter
23	YIL134W	FLX1	6.76	3.77	5.05	FAD carrier protein
24	YPL223C	GRE1	2.55	9.61	4.95	Hydrophilin unknown function; stress induced..
25	YDR472W	TRS31	4.66	5.10	4.88	TRAPP component, ER to Golgi traffic…
26	YHR096C	HXT5	2.40	9.81	4.85	hexose transporter
27	YMR175W	SIP18	3.11	7.38	4.79	Salt-Induced Protein
28	YCR014C	POL4	7.20	3.00	4.65	DNA polymerase IV
29	YOL162W	NA	4.42	4.79	4.60	ORF, member of the Dal5p subfamily…
30	YBL065W	NA	7.76	2.63	4.52	NA
31	YDR070C	NA	2.67	7.07	4.34	Localized to the mitochondria
32	YJL105W	SET4	7.78	2.40	4.32	NA
33	YMR040W	NA	5.49	3.17	4.17	homolog of mammalian BAP31
34	YPR054W	SMK1	4.12	3.92	4.02	MAP kinase
35	YOR055W	NA	4.90	3.26	4.00	NA
36	YIL099W	SGA1	4.34	3.65	3.98	glucoamylase
37	YBL109W	NA	4.08	3.74	3.91	Function unknown…
38	YIL072W	HOP1	6.09	2.50	3.90	DNA binding protein
39	YOL034W	SMC5	4.39	3.32	3.82	Structural maintenance of chromosomes (SMC)
40	YOL037C	NA	4.59	3.15	3.81	NA
41	YKL093W	MBR1	2.73	5.22	3.78	Involved in mitochondrial biogenesis
42	YDR048C	NA	3.65	3.83	3.74	NA
43	YBR284W	NA	3.42	3.97	3.68	Hypothetical ORF
44	YDL024C	DIA3	4.55	2.93	3.65	Involved invasive and pseudohyphal growth…
45	YGR236C	NA	2.77	4.81	3.65	Required for survival at high temperature…
46	YLR312C	NA	2.21	5.91	3.62	Hypothetical ORF
47	YAR050W	FLO1	3.96	3.12	3.52	Lectin-like protein involved in flocculation…
48	YLR174W	IDP2	3.36	3.68	3.51	NADP-dependent isocitrate dehydrogenase
49	YER150W	SPI1	2.12	5.75	3.50	Strongly expressed during stationary phase…
50	YOL084W	PHM7	2.47	4.89	3.48	Unknown function, regulated by phosphate...

Table S1D

Top 50 down-regulated genes *ess1-ts* vs. wild type

	Identifier	UniGene Symbol	*ts* vs. wt at 34°C	*ts* vs. wt 0-estradiol	Combined	UniGene Name
1	YER089C	PTC2	-5.93	-6.47	-6.19	protein phosphatase type 2C
2	YAR031W	PRM9	-5.59	-6.85	-6.19	Pheromone-regulated protein...
3	YGR203W	NA	-4.84	-3.45	-4.09	Probable tyrosine phosphatase…
4	YBR032W	NA	-4.47	-3.53	-3.97	NA
5	YDL198C	GGC1	-3.45	-4.55	-3.96	Mitochondrial GTP/GDP transporter….
6	YDL037C	BSC1	-3.06	-4.79	-3.83	ORF w/high stop codon bypass...
7	YGL209W	MIG2	-2.64	-5.18	-3.70	zinc fingers similar to Mig1p…
8	YNL300W	NA	-2.21	-6.18	-3.69	Hypothetical ORF
9	YIL016W	SNL1	-4.66	-2.54	-3.44	18.3 kDa integral membrane protein
10	YJR025C	BNA1	-4.34	-2.65	-3.39	3-hydroxyanthranilic acid dioxygenase
11	YNL168C	NA	-3.48	-3.14	-3.30	Localized to mitochondria
12	YBR205W	KTR3	-2.82	-3.77	-3.26	alpha-1,2-mannosyltransferase (?)…
13	YER175C	TMT1	-2.56	-3.86	-3.15	Trans-aconitate Methyltransferase 1
14	YHR013C	ARD1	-3.81	-2.44	-3.05	N alpha-acetyltransferase subunit
15	YNL134C	NA	-3.45	-2.69	-3.05	NA
16	YHR201C	PPX1	-3.08	-2.91	-2.99	exopolyphosphatase
17	YJR031C	GEA1	-3.72	-2.39	-2.98	GDP/GTP exchange factor
18	YBR053C	NA	-3.51	-2.47	-2.94	Hypothetical ORF
19	YIL034C	CAP2	-2.57	-3.28	-2.90	capping protein beta subunit
20	YBR206W	NA	-2.44	-3.36	-2.86	NA
21	YNR067C	DSE4	-2.34	-3.50	-2.86	Daughter cell-specific secreted...
22	YPL274W	SAM3	-2.36	-3.45	-2.85	high affinity SAM permease
23	YKL029C	MAE1	-2.87	-2.78	-2.82	malic enzyme
24	YBR261C	NA	-2.78	-2.81	-2.80	Putative SAM-dep. methyltransferase
25	YDR248C	NA	-2.80	-2.79	-2.79	Hypothetical ORF
26	YMR138W	CIN4	-2.56	-2.87	-2.71	GTP-binding protein
27	YNL062C	GCD10	-2.67	-2.74	-2.70	RNA-binding subunit of tRNA MT…
28	YGR277C	NA	-3.03	-2.37	-2.68	Homolog to human PPAT
29	YGR172C	YIP1	-2.82	-2.55	-2.68	Golgi integral membrane protein…
30	YHL009C	YAP3	-2.73	-2.60	-2.66	bZIP protein; transcription factor
31	YPR176C	BET2	-2.80	-2.53	-2.66	geranylgeranyltransferase type II..
32	YHR094C	HXT1	-2.97	-2.30	-2.62	hexose transporter
33	YDR126W	SWF1	-2.35	-2.90	-2.61	Spore Wall Formation
34	YHL011C	PRS3	-2.60	-2.61	-2.61	ribose-phosphate pyrophosphokinase
35	YKL096W	CWP1	-2.68	-2.53	-2.60	cell wall mannoprotein
36	YDR179W	NA	-2.08	-3.25	-2.60	Hypothetical ORF
37	YBR145W	ADH5	-2.15	-3.12	-2.59	alcohol dehydrogenase isoenzyme V
38	YLR128W	NA	-2.21	-3.00	-2.58	Hypothetical ORF
39	YIR017C	MET28	-2.78	-2.35	-2.56	trxn activator Cbf1p-Met4p-Met28p..
40	YJR016C	ILV3	-2.55	-2.52	-2.54	dihydroxyacid dehydratase
41	YPR114W	NA	-2.04	-3.16	-2.54	Hypothetical ORF
42	YBR248C	HIS7	-2.40	-2.66	-2.53	imidazole glycerol P synthase
43	YHR029C	NA	-2.19	-2.80	-2.47	Hypothetical ORF
44	YHR143W	DSE2	-2.19	-2.75	-2.46	Daughter cell-specific secreted...
45	YGL028C	SCW11	-2.25	-2.66	-2.45	glucanase
46	YLR426W	NA	-2.50	-2.35	-2.42	Hypothetical ORF
47	YPL099C	NA	-2.37	-2.39	-2.38	Localized to the mitochondria…
48	YBR194W	NA	-2.50	-2.26	-2.37	Synthetic with Old Yellow Enzyme
49	YNL327W	EGT2	-2.32	-2.42	-2.37	Glycosylphosphatidylinositol (GPI)…
50	YMR132C	JLP2	-2.79	-2.01	-2.37	Hypothetical ORF

Table S2

Top 100 ORFs - with 3' non-coding transcripts: Differential expression (*ess1-ts* vs. wild-type, 34°C) from +25 to +150 bp from the TSS

(5,074 ORFs evaluated)

	ORF	Common name	Adjacent ORF (downstream)	Common name	Fold Up	Aberrant transcripts in *ess1* mutant	Strand	*rrp6* - SAGE (Neil et al., 2009)	Strand	*rrp6* Tiling Array (Xu et al. 2009)	Strand
1	YDR041W	*RSM10*	YDR042C		8.56	*SNR47* RT (1)					
2	YBR118W	*TEF2*	YBR119W	*MUD1*	8.44	E-CBR118/9 (1)	W				
3	YOR271C	*FSF1*	YOR270C	*VPH1*	7.34	E-COR270/1					
4	YML058W	*SML1*	YML057W	*CMP2*	6.96	Readthrough (RT)					
5	YCL005W	*LDB16*	YCL004W	*PGS1*	6.28	E-CCL004/5	W				
6	YMR143W	*RPS16A*	YMR144W		6.20	E-CMR143/4					
7	YLR221C	*RSA3*	YLR220W	*CCC1*	5.94	E-CLR220/1					
8	YLL018C	*DPS1*	YLL018C-A	*COX19*	5.18	RT				CUT248	W
9	YPL081W	*RPS9A*	YPL079W	*RPL21B*	5.17	E-CPL079/81					
10	YFL038C	*YPT1*	YFL039C	*ACT1*	5.15	SUT101	W			SUT101	W
11	YOR279C	*RFM1*	YOR278W	*HEM4*	4.45	*SNR5* RT (1)					
12	YFR033C	*QCR6*	YFR032C-B		4.38	E-CFR032-B/3		CFR033CTa3	W		
13	YLR153C	*ACS2*	YLR152C		4.36	CUT264	W			CUT264	W
14	YHR156C	*LIN1*	YHR155W	*YSP1*	4.32	E-CHR155/6 (*)					
15	YNL103W-A		YNL103W	*MET4*	3.99	SUT334	W			SUT334	W
16	YMR194W	*RPL36A*	SNR11		3.97	E-CMR194/*SNR11*					
17	YER082C	*UTP7*	YER081W	*SER3*	3.89	*SRG1* RT (1)					
18	YJL136C	*RPS21B*	YJL137C	*GLG2*	3.65	E-CJL136/7					
19	YER166W	*DNF1*	YER167W	*BCK2*	3.54	E-CER166/7, TERM					
20	YHL025W	*SNF6*	YHL024W	*RIM4*	3.50	E-CHL024/5					
21	YOR045W	*TOM6*	YOR046C	*DBP5*	3.43	E-COR045/6 (*)					
22	YBL029C-A		YBL030C	*PET9*	3.42	E-CBL029A/30				SUT006	W
23	YNL024C		YNL024C-A		3.36	E-CNL024/A				CUT343	W
24	YNL134C		YNL135C	*FPR1*	3.32	E-CNL134/5				SUT330	W
25	YDR002W	*YRB1*	YDR003W	*RCR2*	3.28	E-CDR002/3				CUT061	W
26	YPR114W		YPR115W	*GCA1*	3.25	E-CPR114/5, RT	W	CPR114WTa2	C		
27	YCR012W	*PGK1*	YCR014W	*POL4*	3.20	E-CCR012/14				CUT045	W
28	YBR249C	*ARO4*	YBR248C	*HIS7*	3.17	CBR249CTa2	W	CBR249CTa2	W	CUT037	W
29	YBR092C	*PHO3*	YBR091C	*MRS5*	3.09	E-CBR091/2, INI, TERM					
30	YOR323C	*PRO2*	YOR322C	*LDB19*	3.08	E-COR322/3					
31	YKL007W	*CAP1*	YKL006C-A	*SFT1*	3.07	E-CKL006A/7, TERM					
32	YHR008C	*SOD2*	YHR007C-A		3.07	CHR008CTa3-A	W	CHR008CTa3-A	W	SUT153	W
33	YLR344W	*RPL26A*	YLR345W		2.99	E-CLR344/5					
34	YGR245C	*SDA1*	YGR244C	*LSC2*	2.91	CGR245CTa3-B	W	CGR245CTa3-B	W		
35	YDR233C	*RTN1*	YDR232W	*HEM1*	2.90	TERM, RT	C				

Table S2

36	YPL198W	*RPL7B*	YPL196W	*OXR1*	2.87	E-CPL196/8					
37	YGL120C	*PRP43*	YGL121C	*GPG1*	2.83	CGL120CTa3 (?) CGL121CTa3 (?)	W	CGL120CTa3 CGL121CTa3	W,W	CUT135	W
38	YHR062C	*RPP1*	YHR061C	*GIC1*	2.81	E-CHR061/2,TERM				SUT159	W
39	YHR155W	*YSP1*	YHR156C	*LIN1*	2.78	E-CHR155/6 (*)					
40	YPR139C	*VPS66*	YPR138C	*MEP3*	2.77	E-CPR138/9, TERM				SUT423,SUT424	W,W
41	YOR046C	*DBP5*	YOR045W	*TOM6*	2.75	E-COR045/6 (*)					
42	YCL028W	*RNQ1*	YCL027W	*FUS1*	2.74	RT (1)	W				
43	YJR104C	*SOD1*	YJR103W	*URA8*	2.74	*URA8* upregulated					
44	YPL136W		YPL135W	*ISU1*	2.74	E-CPL135/6, INI, TERM				SUT400	W
45	YML061C	*PIF1*	YML062C	*MFT1*	2.72	E-CML061/2				SUT293	
46	YIL023C	*YKE4*	YIL024C		2.71	RT	C			CUT698,CUT647	C,C
47	YOR186W		YOR187W	*TUF1*	2.70	E-COR186/7					
48	YKL054C	*DEF1*	YKL055C	*OAR1*	2.68	E-CKL054/5, RT				CUT232,CUT233	W,W
49	YNL002C	*RLP7*	YNL003C	*PET8*	2.68	CNL002CTa2	W	CNL002CTa2	W		
50	YNL016W	*PUB1*	YNL015W	*PBI2*	2.66	CNL016WTa2	C	CNL016WTa2	C	SUT751	C
51	YGR210C		YGR209C	*TRX2*	2.66	E-CGR209/10, INI, TERM					
52	YHR057C	*CPR2*	YHR056W-A		2.65	E-CHRO56A/7 (*)					
53	YMR013W-A		YMR013C	*SEC59*	2.63	YMR013C upregulated					
54	YNL091W	*NST1*	YNL090W	*RHO2*	2.62	TERM, RT				CUT473	C
55	YOR133W	*EFT1*	YOR134	*BAG7*	2.60	COR134WTs2 (?) COR133WTa1-A (?) COR133WTa3-B (?) COR133WTa3-C (?)		COR134WTs2 COR133WTa1-A COR133WTa3-B COR133WTa3-C	W,C,C,C		
56	YDL074C	*BRE1*	SNR63		2.60	E-CDL074/SNR63, TERM				SUT046	W
57	YDL193W	*NUS1*	YDL192W	*ARF1*	2.59	TERM, RT					
58	YJR114W		YJR115W		2.59	RT	W				
59	YLR203C	*MSS51*	YLR201C	*COQ9*	2.58	E-CLR201/3					
60	YDL075W	*RPL31A*	SNR63		2.56	E-CDL075/SNR63, RT					
61	YGR092W	*DBF2*	YGR093W	*DRN1*	2.55	E-CGR092/3				CUT613	C
62	YHR056W-A		YHR057C	*CPR2*	2.53	E-CHRO56A/7 (*)					
63	YPR183W	*DPM1*	YPR184W	*GDB1*	2.51	E-CPR183/4, RT	W	CPR183WTa3	C	CUT923	C
64	YPR043W	*RPL43A*	YPR045C	*MNI2*	2.49	E-CPR043/5 (*)				CUT427	W
65	YBR093C	*PHO5*	YBR092C	*PHO3*	2.47	E-CBR092/3				CUT025	W
66	YOR324C	*FRT1*	YOR323C	*PRO2*	2.45	COR324CTa2	C	COR324CTa2	W	CUT393	W
67	YMR213W	*CEF1*	YMR214W	*SCJ1*	2.44	E-CMR213/4, TERM, RT					
68	YOR013W	*IRC11*	YOR014W	*RTS1*	2.40	E-COR013/4, RT					
69	YHR083W	*SAM35*	YHR084W	*STE12*	2.40	CHR083WTa3	C	CHR083WTa3	C	CUT646	
70	YCL064C	*CHA1*	YCL065W		2.39	TERM	C				
71	YPR045C	*MNI2*	YPR043W	*RPL43A*	2.38	E-CPR043/5 (*)				CUT427	W
72	YGR135W	*PRE9*	YGR136W	*LSB1*	2.36	E-CGR135/6		CGR135WTa3A CGR135WTa3-C	C,C	CUT561,CUT620	C,C
73	YDR349C	*YPS7*	YDR348C		2.33	E-CDR348/9					

Table S2

74	YGR093W	*DRN1*	YGR094	*VAS1*	2.32	E-CGR093/4		CGR093WTa3-A	C	CUT614	C
75	YDL083C	*RPS16B*	YDL084W	*SUB2*	2.32	E-CDL083/4					
76	YBR080C	*SEC18*	YBR079C	*RPG1*	2.31	E-CBR079/80					
77	YML028W	*TSA1*	YML027W	*YOX1*	2.31	RT	W				
78	YOR370C	*MRS6*	YOR369C	*RPS12*	2.29	E-COR369/70					
79	YML125C	*PGA3*	YML126C	*ERG13*	2.29	E-CML125/6, RT					
80	YPL015C	*HST2*	YPL016W	*SWI1*	2.29	E-CPL015/6				SUT820	C
81	YLR388W	*RPS29A*	SNR34		2.28	E-CLR388/SNR34					
82	YHR186C	*KOG1*	YHR185C	*PFS1*	2.28	E-CHR185/6					
83	YOR246C		YOR245C	*DGA1*	2.28	E-COR245/6		COR246CTa2	W		
84	YER164W	*CHD1*	YER165W	*PAB1*	2.27	E-CER164/5		CER165WTs2 CER164WTa3	W,C	CUT570,SUT517	C,C
85	YNL299W	*TRF5*	YNL298W	*CLA4*	2.27	E-CNL298/9, RT	W			CUT798	C
86	YPL036W	*PMA2*	YPL034W		2.27	E-CPL034/6, TERM	W				
87	YLR186W	*EMG1*	YLR187W	*SKG3*	2.26	E-CLR186/7					
88	YMR015C	*ERG5*	YMR014W	*BUD22*	2.26	E-CMR014/5					
89	YMR122W-A		YMR123W	*PKR1*	2.25	E-CMR122A/3		CMR122W-ATa1C CMR121CD1-A	C,C	SUT306,CUT775	W,C
90	YGR156W	*PTI1*	YGR157W	*CHO2*	2.24	CGR156WTa3-B	C	CGR156WTa3-B	C	CUT623,SUT564	C,C
91	YMR142C	*RPL13B*	YMR143W	*RPL16A*	2.23	E-CMR142/3, INI, TERM					
92	YGL198W	*YIP4*	YGL197W	*MDS3*	2.23	E-CGL197/8, TERM, RT		CGL198WTa3	C		
93	YPR070W	*MED1*	YPR071W		2.21	E-CPR070/1, TERM, RT					
94	YLR075W	*RPL10*	YLR077W	*FMP25*	2.21	E-CLR075/7, INI, TERM					
95	YDR315C	*IPK1*	YDR314C	*RAD34*	2.21	E-CDR314/5				CUT080	W
96	YLR056W	*ERG3*	YLR057W		2.20	E-CLR056/7, RT		CLR056WTa3-B	C		
97	YBR256C	*RIB5*	YBR255C-A		2.19	E-CBR255A/6					
98	YER138W-A		YER139C	*RTR1*	2.18	E-CER138A/9					
99	YER048C	*CAJ1*	YER047C	*SAP1*	2.18	E-CER047/8, INI, TERM					
100	YGL031C	*RPL24A*	YGL032C	*AGA2*	2.18	E-CGL031/2, INI, TERM					

(1) confirmed by RT-PCR and/or Northern analysis (this paper); (E-) indicates CUT specific to ess1 mutants (also highlighted in red; (*) transcripts found between two convergent ORFs (will therefore appear more than once in Table); Potential defects in readthrough (RT), initiation (INI) or termination (TERM). Ess1-specific CUTs have been named for the adjacent ORF, using the nomenclature of Neil et al., 2009.

Table S3

Top 100 ORFs - with 5' non-coding transcripts: Differential expression (*ess1-ts* vs. wild-type, 34°C) from -200 to -50 bp from the TSS

(4,367 ORFs evaluated)

	ORF	Common name	Adjacent ORF (upstream)	Common name	Fold Up	Aberrant transcripts in *ess1* mutant	Strand	*rrp6* - SAGE (Neil et al., 2009)	Strand	*rrp6* Tiling Array (Xu et al. 2009)	Strand
1	YHR156C	*LIN1*	YHR157W	*REC104*	6.97	snoRNA , RT (1) ; CUT181	W			CUT181	W
2	YLR152C		YLR153C	*ACS2*	5.94	CUT264, (‡)	W			CUT264	W
3	YOR234C	*RPL33B*	SNR17A		5.45	E-COR234/SNR17A					
4	YMR144W		YMR143W	*RPS16A*	5.45	E-CMR143/4, INI, TERM, (‡)					
5	YOR270C	*VPH1*	YOR271C	*FSF1*	5.36	E-COR270/1, (‡)					
6	YLL018C-A	*COX19*	YLL018C	*DPS1*	5.22	RT, (‡)	C			CUT248	W
7	YDR462W	*MRPL28*	YDR461C-A		5.06	E-CDR461A/2					
8	YOR182C	*RPS30B*	YOR183W	*FVY12*	4.98	E-COR182/3					
9	YPL079W	*RPL21B*	YPL081W	*RPS9A*	4.32	E-CPL079/81, (‡)					
10	YDR156W	*RPA14*	YDR155C	*CPR1*	4.29	E-CDR155/6, (**)		CDR156WD1	W		
11	YPR115W	*GCA1*	YPR114W		4.09	E-CPR114/5, RT	W	CPR114WTa2	C		
12	YCL004W	*PGS1*	YCL005W	*LDB16*	4.08	E-CCL004/5, RT, (‡)	W				
13	YJR145C	*RPS4A*	YJR147W	*HMS2*	3.91	E-CJR145/7	W			SUT650	C
14	YGL031C	*RPL24A*	YGL030W	*RPL30*	3.85	E-CGLO30/1, INI, TERM (**)					
15	YHR041C	*SRB2*	YHR042W	*NCP1*	3.67	E-CHR041/2, (**)	W			SUT156,CUT642	W,C
16	YHR021C	*RPS27B*	YHR021W-A	*ECM12*	3.66	CHR021W-AD4	W	CHR021W-AD4	W		
17	YGL189C	*RPS26A*	YGL188C-A		3.58	E-CGL188A/9	W				
18	YKR094C	*RPL40B*	YKR095W	*MLP1*	3.56	CKR094CD1	W	CKR094CD1	C	SUT242	W
19	YCR013C		YCR014C	*POL4*	3.36	CUT045	W			CUT045	W
20	YLR432W	*IMD3*	YLR431C	*ATG23*	3.30	CLR432WD2	W	CLR432WD2	W		
21	YAL003W	*EFB1*	YAL005C	*SSA1*	3.26	E-CAL003/5					
22	YGR149W		YGR148C	*RPL24B*	3.16	E-CGR148/9					
23	YIL069C	*RPS24B*	YIL068C	*SEC6*	3.16	E-CIL068/9					
24	YDR234W	*LYS4*	YDR233C	*RTN1*	3.13	CDR233CD3-A CDR234WD2	C,W	CDR233CD3-A CDR234WD2	C,W		
25	YJR148W	*BAT2*	YJR147W	*HMS2*	3.10	CJR147WTa3	C	CJR147WTa3	C	SUT650	C
26	YIL051C	*MMF1*	YIL050W	*PCL7*	3.07	CIL050WD1-B CIL051CD1-B, (**)	W,C	CIL050WD1-B CIL051CD1-B	W,C		
27	YPL206C	*PGC1*	YPL204W	*HRR25*	3.07	CPL206CD1, (**)	C	CPL206CD1	C	CUT886	C
28	YGR148C	*RPL24B*	YGR149W		3.06	E-CGR148/9 (**)					
29	YDR233C	*RTN1*	YDR234W	*LYS4*	3.02	CDR233CD3-A CDR234WD2; (**)	C,W	CDR233CD3-A CDR234WD2	C,W		
30	YBL030C	*PET9*	YBL029C-A		2.94	E-CBL029C/30, (‡)	W			SUT006	W
31	YPL233W	*NSL1*	YPL234C	*TFP3*	2.87	E-CPL233/4	W				

Table S3

32	YNL015W	*PBI2*	YNL016W	*PUB1*	2.85	CNL016WTa2, (‡)	C	CNL016WTa2	C	SUT751	C
33	YDL082W	*RPL13A*	YDL083C	*RPS16B*	2.83	E-CDL082/3, (**)					
34	YJL137C	*GLG2*	YJL136C	*RPS21B*	2.81	E-CJL136/7, (‡)					
35	YBR248C	*HIS7*	YBR249C	*ARO4*	2.77	CBR249CTa2, (‡)	W	CBR249CTa2	W	CUT037	W
36	YGR244C	*LSC2*	YGR245C	*SDA1*	2.77	CGR245CTa3-B, (‡)	W	CGR245CTa3-B	W		
37	YDR471W	*RPL27B*	YDR470C	*UGO1*	2.74	E-CDR470/1					
38	YNL298W	*CLA4*	YNL299W	*TRF5*	2.74	E-CNL298/9, RT, (‡)	W			CUT798	C
39	YNL300W		YNL301C	*RPL18B*	2.72	E-CNL300/1, RT, (**)	W			SUT742	C
40	YHR042W	*NCP1*	YHR041C	*SRB2*	2.72	E-CHR041/2, (**)	W			SUT156,CUT642	W,C
41	YDR155C	*CPR1*	YDR156W	*RPA14*	2.71	E-CDR155/6, (**)		CDR156WD1	W		
42	YEL009C	*GCN4*	YEL007W		2.70	CEL007WD1-C CEL009CD2	W,C	CEL007WD1-C CEL009CD2	W,C		
43	YCL027W	*FUS1*	YCL028W	*RNQ1*	2.68	RT, (‡) (1)	W				
44	YBR119W	*MUD1*	YBR118W	*TEF2*	2.65	E-CBR118/9, (‡) (1)	W				
45	YPL143W	*RPL33A*	SNR17B		2.63	E-CPL143/SNR17B					
46	YPR144C	*NOC4*	SNR45		2.63	CUT916	C			CUT916	C
47	YJR105W	*ADO1*	YJR104C	*SOD1*	2.62	E-CJR104/5				SUT217,SUT645	W,C
48	YGL121C	*GPG1*	YGL120C	*PRP43*	2.62	CGL120CTa3 (?) CGL121CTa3 (?), (‡)	W	CGL120CTa3 CGL121CTa3	W,W	CUT135	W
49	YPL204W	*HRR25*	YPL206C	*PGC1*	2.61	E-CPL204/6, (**)				CUT886	C
50	YNL135C	*FPR1*	YNL134C		2.60	E-CNL134/5, (‡)				SUT330	W
51	YER009W	*NTF2*	YER008C	*SEC3*	2.60	E-CER008/9, (**)					
52	YGR214W	*RPS0A*	YGR213C	*RTA1*	2.60	E-CGR213/4				CUT162	W
53	YBL071W-A	*KTI11*	YBL071C-B		2.59	E-CBL071A/B	W				
54	YGR209C	*TRX2*	YGR210C		2.58	E-CGR209/10, INI, TERM, (‡)					
55	YER058W	*PET117*	YER057C	*HMF1*	2.56	E-CER057/8		CER057CD1	C	SUT092	W
56	YCL057C-A		YCL057W	*PRD1*	2.55	CCL057WD1, (**)	W	CCL057WD1	W		
57	YBR091C	*MRS5*	YBR092C	*PHO3*	2.55	E-CBR091/2, INI, TERM, (‡)					
58	YJL190C	*RPS22A*	YJL189W	*RPL39*	2.54	E-CJL189/90				SUT617	C
59	YEL044W	*IES6*	YEL046C	*GLY1*	2.53	E-CEL044/6		CEL046CD1 CEL046CD2	C,C		
60	YKL006W	*RPL14A*	SNR87		2.49	E-CKL006/SNR87		CKL006WD1-A	W		
61	YNL003C	*PET8*	YNL002C	*RLP7*	2.48	CNL002CTa2, (‡)	W	CNL002CTa2	W		
62	YDR003W	*RCR2*	YDR002W	*YRB1*	2.48	E-CDR002/3, (‡)				CUT061	W
63	YKL150W	*MCR1*	YKL151C		2.48	E-CKL150/1					
64	YBR173C	*UMP1*	YBR175W	*SWD3*	2.47	E-CBR173/5					
65	YIL050W	*PCL7*	YIL051C	*MMF1*	2.47	CIL050WD1-B CIL051CD1-B CIL051CD2, (**)		CIL050WD1-B CIL051CD1-B CIL051CD2	W,C,C		
66	YNL096C	*RPS7B*	YNL095C		2.44	E-CNL095/6				SUT334	W
67	YLR172C	*DPH5*	YLR173W		2.42	CLR172CTa1	W	CLR172CTa1	W	SUT268	W
68	YMR240C	*CUS1*	YMR241W	*YHM2*	2.38	E-CMR240/1	C	CMR241WD1	W		

Table S3

69	YMR142C	*RPL13B*	YMR143W	*RPS16A*	2.37	E-CMR142/3, INI, TERM, (‡)						
70	YOL154W	*ZPS1*	YOL155C	*HPF1*	2.37	E-COL154/5 (1)						
71	YOR312C	*RPL20B*	YOR313C	*SPS4*	2.36	E-COR312/3						
72	YDR510W	*SMT3*	YDR508C	*GNP1*	2.34	E-CDR508/10		CDR508CD3	C			
73	YBL087C	*RPL23A*	YBL086C		2.34	E-CBL086/7						
74	YCL057W	*PRD1*	YCL057C-A		2.33	CCL057WD1, (**)	W	CCL057WD1	W			
75	YCR032W	*BPH1*	SNR189		2.32	CCR032WD1	W	CCR032WD1	W	CUT048	W	
76	YNL090W	*RHO2*	YNL091W	*NST1*	2.31	TERM, RT, (‡)	W					
77	YFR032C-B		YFR033C	*QCR6*	2.30	E-CFR032B/3, (‡)	W	CFR033CTa3	W			
78	YFL031W	*HAC1*	YFL033C	*RIM15*	2.30	E-CFL031/3		CFL031WD2 CFL033CD2	W,C			
79	YPR184W	*GDB1*	YPR183W	*DPM1*	2.29	E-CPR183/4, RT, (‡)	W	CPR183WTa3	C	CUT923	C	
80	YNL240C	*NAR1*	YNL239W	*LAP3*	2.28	E-CNL239/40, (**)	W			SUT324	W	
81	YBR083W	*TEC1*	YBR082C	*UBC4*	2.28	E-CBR082/3	W	CBR082CD1-B CBR082CD1-C	C,C	CUT453	C	
82	YGR027C	*RPS25A*	YGRWDELTA11		2.27	E-CGR027/DELTA11		CGR027CD1-A CGR027CD1-B	C,C	CUT606	C	
83	YML027W	*YOX1*	YML028W	*TSA1*	2.26	RT, (‡)	W					
84	YCL021W-A		YCLCDELTA1		2.26	E-CCL021A/DELTA1, RT	W	CtE(UUC)CD2	C			
85	YNL239W	*LAP3*	YNL240C	*NAR1*	2.25	E-CNL239/40, (**)	W			SUT324	W	
86	YHR204W	*MNL1*	YHR203C	*RPS4B*	2.25	E-CHR203/4, RT	W					
87	YLR345W		YLR344W	*RPL26A*	2.23	E-CLR344/5, (‡)						
88	YOL039W	*RPP2A*	YOL040C	*RPS15*	2.23	E-COL039/40, (**)						
89	YNL301C	*RPL18B*	YNL300W		2.23	E-CNL300/1, RT, (**)	W			SUT742	C	
90	YDL083C	*RPS16B*	YDL082W	*RPL13A*	2.21	E-CDL082/3, (**)						
91	YML007W	*YAP1*	YML007C-A		2.21	E-CML007/A				SUT296/uORF	W	
92	YER008C	*SEC3*	YER009W	*NTF2*	2.20	E-CER008/9, (**)				SUT330	W	
93	YOL040C	*RPS15*	YOL039W	*RPP2A*	2.20	E-COL039/40, (**)						
94	YLL048C	*YBT1*	YLL046C	*RNP1*	2.20	E-CLL046/8	C	CLL046CTa3-B	W			
95	YLR350W	*ORM2*	YLR349W		2.20	E-CLR349/50				SUT708	C	
96	YBR048W	*RPS11B*	YBR047W	*FMP23*	2.19	E-CBR047/8		CBR047WTa3	C			
97	YKL103C	*LAP4*	YKL101W	*HSL1*	2.17	E-CKL101/3		CKL103CD3	C	CUT229	W	
98	YGR157W	*CHO2*	YGR156W	*PTI1*	2.16	CGR156WTa3-B, (‡)	C	CGR156WTa3-B	C	CUT623,SUT564	C,C	
99	YOR052C		YOR053W		2.16	E-COR052/3						
100	YOR322C	*LDB19*	YOR323C	*PRO2*	2.15	E-COR322/3, (‡)						

(1) Confirmed by RT-PCR and/or Northern analysis (this paper); (E-) indicates CUT specific to ess1 mutants (also highlighted in red); (**) transcripts found between two divergent ORFs (will therefore appear more than once in Table); (‡) transcripts also identified in 3′ analysis (Table S2); Potential defects in readthrough (RT), initiation (INI) or termination (TERM). Ess1-specific CUTs have been named for the adjacent ORF, using the nomenclature of Neil et al., 2009.

Table S4. *Saccharomyces cerevisiae* strains used in this study

Strain name	Genotype	Source
W303-1A	*MAT***a** *ura3-1 trp1-1 leu2-3,112 can1-100 ade2-1 his3-11,15*	Thomas and Rothstein (1989)
W303-1B	*MATα ura3-1 trp1-1 leu2-3,112 can1-100 ade2-1 his3-11,15*	Thomas and Rothstein (1989)
YGD-ts22	*MAT***a** *ura3-1 trp1-1 leu2-3,112 can1-100 ade2-1 his3-11,15 ess1^{H164R}*	Wu et al., (2000)
YSB2039	*MAT***a** *ura3-1 trp1-1 leu2-3,112 can1-100 ade2-1 his3-11,15 PCF11-TAP*	S. Buratowski
YSB2040	*MAT***a** *ura3-1 trp1-1 leu2-3,112 can1-100 ade2-1 his3-11,15 ess1^{H164R} PCF11-TAP*	S. Buratowski (unnpublished)
YXW137	*MAT***a** *ura3-1 trp1-1 leu2-3,112 can1-100 ade2-1 his3-11,15 ess1Δ::HIS* (pRS315-GAL1-ESS1)	Gemmill et al., (2005)
YXW138	*MAT***a** *ura3-1 trp1-1 leu2-3,112 can1-100 ade2-1 his3-11,15 ess1Δ::HIS* (pRS315-GAL1-H164R)	Gemmill et al., (2005)
YJM1	*MAT***a** *ura3-1 trp1-1 leu2-3,112 can1-100 ade2-1 his3-11,15 srb10::TRP1*	Wilcox et al., (2004)
YJM2	*MAT***a** *ura3-1 trp1-1 leu2-3,112 can1-100 ade2-1 his3-11,15 ess1^{H164R} srb10::TRP1*	Wilcox et al., (2004)
CBW22	*MAT***a** *ura3-1 trp1-1 can1-100 ade2-1 his3-11,15 ess1ΔHIS3 srb10::TRP1*	Wilcox et al., (2004)
46a	*MAT***a** *cup1Δ ura3 his3 trp1 lys2 ade2 leu2*	Steinmetz and Brow, (1996)
46a nrd1-5	*MATα cup1Δ ura3 his3 trp1 lys2 ade2 leu2 nrd1-5*	Steinmetz and Brow, (1996)
YJC1412	*MAT***a** *ade2 can1-100 his3-11,15 leu2-3,112 trp1-1 ura3-1*	Conrad et al., (2000)
YJC1098	*MAT***a** *ade2 can1-100 his3-11,15 leu2-3,112 trp1-1 ura3-1 nab3-11*	Conrad et al., (2000)
NA67	*MATα ura3-1 leu2-3,112 trp1Δ his3-11,15 ade2-1 pcf11-9*	Amrani et al., (1997)
BY4741	*MAT***a** *his3Δ1 leu2Δ0 met15Δ0 ura3Δ0*	Open Biosystems
Ess1-TAP	*MAT***a** *his3Δ1 leu2Δ0 met15Δ0 ura3Δ0 ESS1-TAP::HIS3*	Open Biosystems

Table S5. Oligonucleotides used in this study

Name	Locus	Sequence (5'->3')	Use
OW547	SNR5-Forward (F)	GGT TCG CTC TAG GTG TAC ATA TC	Intergenic PCR
OW548	SNR5-Reverse (R)	AAG CGG TAC GAA TAT GGG TTC	"
OW551	SNR10-F	GTA GTT GGA TTG ACG CAT G	"
OW552	SNR10-R	CTA CAC AAT CTC TGC TCA TTA C	"
OW561	SNR13-F	GCT CGA GTT GCT GTT TGG CTT	"
OW562	SNR13-R	TTG TTG GTC AGA TGC GCT TGG	"
OW545	SNR33-F	AAA GCC TAG CTT TTA CAC CGG	"
OW546	SNR33-R	GTA TCC GTC CAT ATA TGT C	"
OW563	SNR50-F	CCT TTA CAG AAC CGC TAC AC	"
OW564	SNR50-R	TGG TCA TGC TAG GGA TAT AG	"
OW559	SNR60-F	GAG ACC ATT GTG GAG CGA TTT	"
OW560	SNR60-R	ATG TCC CCT GTA AGC AAG TGT	"
OW553	SNR68-F	GTT GGA TTT ATC ATG ATG AGC	"
OW554	SNR68-R	CTA ATG GAT GCA CTA CCA ATG	"
OW543	SNR71-F	GAT AAT CTA AGT CGG CTA AG	"
OW544	SNR71-R	GAA TGA CCA TGC TAA GCT GC	"
OW565	SNR79-F	CTC AAG ACT ACA ACG GTA TC	"
OW566	SNR79-R	AAC TCT GGA AGG TCA TCT AC	"
OW549	SNR82-F	CCC ACA GTC TAT AGT TTG ATA G	"
OW550	SNR82-R	GCT TTC CTT CGT AGA CGA TTC	"
OW501	PYK1-F	CTC TCT TGT TTC TAT TTA CAA GAC ACC AAT C	"
OW502	PYK1-R	CGG AGA TGA CCT TGG TGA TGT TC	"
OW513	SNR5-F	TTG CAG GAT CCT TCA GGA TAA G	Northern probes (PCR)
OW514	SNR5-R	AGC TGA CTA CAG CAC AAC CCA AC	"
OW511	HEM4-F	GGT AAA ATA GAC CTT GCT CGA G	"
OW528	HEM4-R	ACG GAG ATG AAG GGG AGA CCA AAA TC	"
OW521	SNR13-F	ATG GCA TCT CAA ATC GTC TC	"
OW522	SNR13-R	TCC GTG TCT CTT GTC CTG CAA AG	"
OW587	TRS31-F	TAT CAC CAT CCA TAA TAC TGG AG	"
OW588	TRS31-R	TGA GAT GAT ATC AGC CAA ATC TC	"
OW611	SNR51-F	TGA TAA AAG AGA CTG TTG CG	"
OW612	SNR51-R	TAC ATA GGG TGC AAG ATT AG	"
OW585	YPR091C-F	TCT CGC AGT TTA CTT GCT TGG C	"
OW586	YPR091C-R	GTT GTG AAG GCC TTC TTG GTA C	"
OW599	SNR60-F	CTG ACA TAC AAC AGG TGT TG	"
OW600	SNR60-R	GCC CTT CTC CAA TTA CAA GC	"
OW597	UBX6-F	GAC CCT CAA AGG AAG TGA ATT ACA G	"
OW598	UBX6-R	CAT GAT GGA AGA ACA ACC ACG TTG	"
OW515	SNR82-F	ACG GCC CTC TAT TAA TTT GCT C	"
OW516	SNR82-R	CGC TCA TAT GAC AAG ATA TAG GG	"
OW581	USE1-F	GTT GAC AGG ACA CAT AAT AGC	"
OW582	USE1-R	GGA GAA TTC TGC AGC CTA TAC	"
OW595	SNR33-F	CGG AAC GGT ACA TAA GAA TA	"
OW596	SNR33-R	CAG ATA AAC AAG CTC AGT AG	"
OW577	YCR015C-F	ACA ATT GCA GTA ACC AGA AGC G	"
OW578	YCR015C-R	CGG AGA TAG AAG AAT AGT GCA AG	"
OW658	FUS1-F	TGC AGA CGA CAA CAA CTG TG	"
OW659	FUS1-R	TGT CTT CCC TAA TTG GAC GC	"
OW858	GRE1-F	TGA-CAT TTG ATC GCA AGT TC	"

OW859	GRE1-R	TAT TCA TCG TTT CCT GAC CCA	“
OW932	NMR026W-F	CAA TTT TAT CAA GAC CGC AC [1]	“
OW933	NMR026W-R	TAA ACG TTA GCG TGT TCT TG [1]	
OW646	ZPS1-F	CAA CTC TAC TGC TGA GTT AC	“
OW647	ZPS1-R	ACA GAA GCA CTG TAA ACG TC	“
OW666	YGR277-F	TAG TGC TAC TTT GCA GAG GA	“
OW667	YGR277-R	GAC TTA AGT AGG CGT CTG AT	“
OW856	IMD2-F	GCT GAA CAT TTA ACC GGA GAA TCT	“
OW857	IMD2-R	CTT AAT GGA TCC TTT GTC AAC GAC	“
OW862	SRG1-F	ACT CAC AAT CGA GTA ATG CCT	“
OW863	SRG1-R	GAA TTT CCT TAT CCT CTG CTC	“
OW864	SER3-F	CGA AGA GCA AGG TTA CCA AGT C	“
OW865	SER3-R	GCA CAG TGT TCT CTT GGT CGT A	“
OW650	MUD1-F	ATC CCA ACA ACA AGT ATG CC	“
OW651	MUD1-R	GCA AAT CCT ATG GTA ACG TC	“
OW656	SMK1-F	TAC CAG AGC CAT AAA TGT GG	“
OW657	SMK1-F	GGA TTC ATA GGT GAA GTC GA	“
OW681	SNR5-HEM4 1-F	AGG CTG ACG TTA ATA GGA AC	Chromatin Ip
OW682	1-R	ATC TCT TAG GGC TCC TAC TG	“
OW513	2-F	TTG CAG GAT CCT TCA GGA TAA G	“
OW683	2-R	GTC TAC TTC CAG CCA TTT GC	“
OW547	3-F	GGT TCG CTC TAG GTG TAC ATA TC	“
OW514	3-R	AGC TGA CTA CAG CAC AAC CCA AC	“
OW511	4-F	GGT AAA ATA GAC CTT GCT CGA G	“
OW548	4-R	AAG CGG TAC GAA TAT GGG TTC	“
OW686	SNR47-YDR042C 1-F	ATC AGA ACT GTC TCC GAA CA	“
OW687	1-R	ATG ACC GTA TGG AAG ACG TA	“
OW613	2-F	ACA TTC TCT TGG CGA GTG AT	“
OW688	2-R	ACC TAT AAA GGA TTC GGA CG	“
OW541	3-F	CCT TTA TAG GTG GAA ACA AAC	“
OW532	3-R	GCT ACT CTG ATT TAC GTT ACC GC	“
OW689	4-F	TCG GGA TAA CAA AGC GTA CT	“
OW542	4-R	CTC TTA GAG ACC TAG TCG T	“
OW573	5-F	GCG AAT CAA CAA CAG CTA AC	“
OW690	5-R	CAT TCT TGG TAG CAG ATA TG	“
OW709	6-F	TAT TAA GCG GTA TGC AGT ACC	“
OW710	6-R	GAT GGC AAT CCT ATA ATT ACG C	“
OW595	SNR33-YCR015C-POL4 1F	CGG AAC GGT ACA TAA GAA TA	“
OW669	1-R	TAG TGC TTG ATA TCA CAT CC	“
OW757	2-F	GCT TAA TGC CCT CTT TGT AC	“
OW758	2-R	ATC GAT TGT CCA CAC ACT TC	“
OW545	3-F	AAA GCC TAG CTT TTA CAC CGG	“
OW596	3-R	CAG ATA AAC AAG CTC AGT AG	“
OW577	4-F	ACA ATT GCA GTA ACC AGA AGC G	“
OW546	4-R	GTA TCC GTC CAT ATA TGT C	“
OW707	5-F	GCT AAT AAA CCC GCA AGA AAA TC	“
OW708	5-R	AGA GTC CCA GGA TTT CAC AAG GTA G	“
OW670	6-F	TGC CTA CCT TGT GAA ATC CTG	“
OW578	6-R	CGG AGA TAG AAG AAT AGT GCA AG	“
OW579	7-F	CAT GCG ACC TGT TAG ACA AAT C	“
OW671	7-R	GAC CAC TTC CTT ACG GCT AGA TT	“
OW712	SNR82-USE1 1-F	GTC CTA GAG ATA TTA TAA AAC GG	“
OW713	1-R	CCA CTA ACA CAA ATT ACT TGA AC	“

OW754	2-F	TGG CTC TTC AAC ACA TTT CAA	“
OW694	2-R	GAA GCT TAA GGA TAA TCA GAC G	“
OW549	3-F	CCC ACA GTC TAT AGT TTG ATA G-	“
OW715	3-R	ATC CAG ACC GAC ATC TGT AAC	“
OW581	4-F	GTT GAC AGG ACA CAT AAT AGC	“
OW550	4-R	GCT TTC CTT CGT AGA CGA TTC	“
OW696	5-F	GTG ACG ACA ATA AGG TCT CAG	“
OW697	5-R	TCA ACT CCA TAA CAG CTT CGC	“
OW698	6-F	GAT TCT CGG ACT GGT GTT TAC	“
OW582	6-R	GGA GAA TTC TGC AGC CTA TAC	“
OW761	MUD1 (*NBR024W*) 1-F	ACT GCT CAC ATT GCT TGT AG	“
OW762	1-R	CAG TCT TGT CAA CAG ACT TG	“
OW866	2-F	CTG CTC AAA AGG CTG CTA AGA A	“
OW867	2-R	TGA GGC CGT CTT TTG TTG AT	“
OW868	3-F	AAG CTG CTA TCA ACA AAA GAC GG	“
OW869	3-R	CGA CGG ATT AAT GGC ATA CTT G	“
OW650	4-F	ATC CCA ACA ACA AGT ATG CC	“
OW763	4-R	TCT GCT TCT TCT TGA GTG AC	“
OW651	5-F	GCA AAT CCT ATG GTA ACG TC	“
OW764	5-R	ATC GCA GAA ACC TCT TAA GC	“
V-1	Intergenic control -F	GGC TGT CAG AAT ATG GGG CCG TAG [2]	“
V-2	(chr. V) -R	CAC CCC GAA GCT GCT TTC ACA ATA C [2]	“
OW917	GRE1-F	CAG GTA TGG GTT TGA GGA TGT TCT	qRT-PCR (CUTs)
OW918	GRE1-R	AAA TGA CGA AGC CCA AAA CG	“
OW932	NMR026W-F	CAA TTT TAT CAA GAC CGC AC [1]	“
OW933	NMR026W-R	TAA ACG TTA GCG TGT TCT TG [1]	
OW789	NGR060W-F	TCT GAA GCA CAA AAG GGA GC	“
OW790	NGR060W-R	ATA CGT TTG TCC CTA AGT GC [3]	“
OW787	NEL025C-F	GCA AAG ATC TGT ATG AAA GG [3]	“
OW788	NEL025C-R	CGC AGA GTT CTT ACC AAA CG [3]	“
OW787	NEL025C-F	GCA AAG ATC TGT ATG AAA GG	“
OW929	NEL025C-R	GCG TCT TTC CTG TTT ATG AG	“
OW903	NGR047W-F	ACA GGA AAA CAG CAA TGA CCA	“
OW904	NGR047W-R	CTA AAA TCT TTG CAT TTG TCA TCC	“
OW909	gGR12-F	CGT TGC CAA CTG GTA CAT TT	“
OW910	gGR12-R	AGA TAG TTT TAC AGG CGG TTC C	“
OW915	NPR021W-F	AGG ATG ATG TTG GTT TGA CCG T	“
OW916	NPR021W-R	ATA CCG CCA TTC TCC TGC TTA	“
OW907	uZPS1-F	CTT TTC CAG ATC ACG AAT CTG TTG	“
OW908	uZPS1-R	GTT GCA AAG ATG ATA GAT TTG CC	“
OW923	dYGR277-2-F	AAC GTG TGA CCT TAT CAT TTC CC	“
OW924	dYGR277-2-R	GGC GGT GTA TAA GGA AGA ACA A	“
OW781	SRG1-F	GCC AAG CTA TGT GCA AAT ATC AC	“
OW918	SRG1-R	TTT CCT TAT CCT CTG CTC CCT	“
OW783	SER3-F	TGA CAA GCA TTG ACA TTA ACA AC	“
OW784	SER3-R	TTT TCG ATC AAC TCT TCC TCG G	“
OW927	NBR024-F	TGG TGT TTT CTT GCC CAT CA	“
OW902	NBR024-R	ACG CTG ACA TGG TTT CTT TAG GT	“
OW785	ACT1-F	CTG AGG TTG CTG CTT TGG TTA TT	“
OW786	ACT1-R	GGG CAA CTC TCA ATT CGT TGT A	“

[1] after Thompson and Parker (2007)

[2] after Komarnitsky et al. (2006)

[3] after Wyers et al. (2005)

Supplemental Figure Legends

Figure S1. Expression array analyses of *ess1* mutants. (**A**) Scatterplots of *ess1*^{H164R} temperature-sensitive mutants (Wu et al., 2000) vs. wild type reveal only a small fraction of the genome is affected. Control panels (upper row) reveal a tight distribution of data points along the diagonal, as expected. Comparisons between the *ess1*^{H164R} mutant and wild-type were done at two temperatures (24°C and 34°C), and as expected a greater spread in the distribution away from the diagonal (in yellow) is apparent at restrictive temperature (34°C). Data points above the diagonal (in red) are elevated in *ess1*^{H164R} cells relative to wild type, while points below the diagonal (in green) are reduced in mutants. (**B**) A similar analysis was done using an *ess1*Δ::*HIS3* shutoff strain (YXW138) expressing the *ess1*^{H164R} allele from the *GAL1* promoter under control of a GAL4-estrogen receptor-VP16 fusion activator (Gemmill et al. 2005). In absence of added hormone (0 β-estradiol), the strain produces a very low level of the Ess1(H164R) protein, whereas at 100 nM estradiol, the mutant protein is overproduced to levels supporting nearly normal growth (Gemmill et al., 2005). Cells were grown at 30°C. The control cells (YXW137) were *ess1*Δ::*HIS3* with *ESS1* under control of the *GAL1* promoter as above. As expected, the number of genes affected in the absence of estradiol is greater than that with 100 nM estradiol. (**C**) Venn diagrams representing the extent of overlap in the gene sets identified in the two experiments described in A and B, above. P-values based on the hypergeometric distribution indicate a highly significant overlap. The top 50 genes in common in each category are listed in **Table S1C,D.** (**D**) Venn diagrams representing genes in common among the top up-regulated genes identified by microarray analysis of *ess1*^{H164R} mutants (Affymetrix YG98S microarray; this study) and *ssu72* mutants (printed array; Ganem et al., 2003). P-values were calculated using N=5000 genes for each (out of 6871 for *ess1*^{H164R} and 5885 for *ssu72* mutants). (**E**) Venn diagrams representing genes in common among the top up-regulated genes identified by microarray analysis of *ess1*^{H164R} mutants (Affymetrix YG98S microarray; this study) and *nab3-11* (Affymetrix YG98S microarray; Arigo et al., 2006) mutants. P-values were calculated using N=5000 genes for each (out of 6871 for *ess1*^{H164R} mutants and at least 5000 for *nab3-11* mutants).

Figure S2. Average differential expression *ess1* mutants vs. wild type. (**A**) Readthrough at the 3' end of snoRNA genes. Average differential expression of *ess1*^{H164}/wild type was computed by comparing tiling array data at each position within a 600 bp window encompassing +/- 300 bp from the predicted 3' end of 29 snoRNA genes. Polycistronic and snoRNA genes with convergent ORFs were excluded. (**B**) Readthrough at the 3' end of non-snoRNA genes. Average differential expression for 5,074 ORFs aligned relative to the transcription termination site (TTS) (Nagalakshmi *et al.*, 2008). ORFs transcribed from opposing strands with overlapping

3' UTRs were excluded, as were ORFs affected by upstream snoRNA genes. (**C**) Increased 5' transcription in *ess1*^{H164} cells may identify new upstream regulatory RNAs (uRNAs). Average differential expression for 4,367 ORFs aligned relative to the transcription start site (TSS) (Nagalakshmi et al., 2008). Genes with overlapping (divergent) promoters and genes downstream of snoRNA genes were excluded. Colored lines in **B** and **C** represent three independent controls of the average differential expression of 600 bp segments from 5,074 and 4,367 random locations across the genome, respectively.

Figure S3. Tiling array data indicating readthrough of snoRNAs in *ess1* mutants. Data are displayed using Integrated Genome Browser (IGB). **(A-D)** Examples of different patterns of transcription readthrough of snoRNA genes in *ess1*^{H164R} mutants. (**A**) Readthrough continues through the downstream ORF (*USE1*). (**B**) Readthrough stops at the 5' end of *YTM1*. (**C**) Readthrough proceeds through an ORF (YPR092W) on the opposite strand. (**D**) The *SNR52* gene is transcribed by RNA pol III (instead of pol II) and as expected, does not exhibit readthrough in *ess1* mutant cells.

Figure S4. Average differential expression in selected regions, *ess1* mutants vs. wild type. (**A**) Rank ordered average differential expression in the region +25 through +150 of 3' TTS for each gene in the processing set of Fig. S2B. This interval was chosen for analysis because it appears to be most representative of 3' differential expression in Fig. S2B. Due to missing probes, one gene did not have data in the selected region, thus data for 5,073 genes was used. Genes with the most pronounced differential expression in the region appear at the left-most portion of the plot and the majority of genes show little or no effect. The rapidly decreasing slope of the curve indicates a relatively few number of genes account for the shape of Fig. S2B and its y-axis scale. (**B**) Rank ordered average differential expression in the region -250 through -50 to 5' TSS for each gene in the processing set of Fig. S2C. This interval was chosen for analysis because it appears to be most representative of 5' differential expression in S2C. Similar to (**A**), high differential expression of genes at left-most portion of the plot shows that a relatively small number of genes account for the shape of Fig. S2C and its y-axis scale.

Figure S5. Novel 3' and 5' sense and antisense transcripts revealed by bioinformatic analysis of tiling array data from *ess1* mutants. (**A-E**) Examples of aberrant 3' transcription in *ess1*^{H164R} mutants among genes rank ordered among the top 50 in Fig. S4A and listed in Table S2. (**F-J**) Examples of aberrant 5' transcription in *ess1*^{H164R} mutants among genes rank ordered among the top 50 in Fig. S4B and listed in Table S3. (**A**) Probable transcription readthrough of the *SML* gene in *ess1*^{H164R} mutants. (**B**) Example of a previously identified antisense CUT (Neil et al., 2009) and (**C**) an antisense SUT (Xu et al., 2009) that are also revealed in *ess1*^{H164R} mutants.

(**D,E**) Examples of probable 3' antisense CUTS that are specific to *ess1*^{H164R} mutants (i.e. not previously identified in *rrp6*Δ or other Nrd1-related mutant backgrounds). Probable 5' sense (**F,G**) and antisense (**H,I**) CUTs that are specific to *ess1*^{H164R} mutants. (**J**) Previously identified divergent CUT (CDR050cTs2/CUT497) and SUT (CDR051cTa3-A/SUT056) transcripts (Neil et al., 2009; Xu et al., 2009) also revealed in *ess1*^{H164R} mutants .

Figure S6. Chromatin Ip for localization of Nrd1 and Pcf11 on CUT and ncRNA loci. (A,D,F) Schematics showing location of PCR products used for ChIP. (**B,D**) Overexpression of Ess1 reduces recruitment of Nrd1 to terminator regions of two snoRNA genes. (**F**) Nrd1 ChIP at a CUT locus showing increased recruitment of Nrd1 in *ess1*^{H164R} mutant cells relative to wild type. (**G**) Pcf11 ChIp at the same locus as in B, shows decreased recruitment of Pcf11 in *ess1*^{H164R} mutant cells relative to wild type. All ChIP data are expressed as fold increase over a chromosome V control locus. Results in this figure are consistent with a model in which Ess1 is required for release of Nrd1 from the CTD and subsequent binding of Pcf11 (see Fig. 7 in main text). Error bars are standard deviation from the mean of at least 3 biological replicates.

Figure S7. Tiling array data identifying CUTs and uRNAs in *ess1* mutants. (**A, B**) Tiling results along with other data (see text), suggest the presence of novel CUT RNAs in *ess1*^{H164R} mutant cells. Dotted lines represent the approximate locations of these putative CUTs. (**C-F**) Examples of genes known to be regulated by non-coding upstream regulatory RNAs (uRNAs). Tiling profiles shown here for *ess1*^{H164R} mutant cells are consistent with upstream transcripts reading through into the downstream ORFs as in *nrd1*, *sen1*, and *nab3* mutants. (**G**) Venn diagram representing the overlap between potential CUTs identified as SAGE tags, which are up-regulated in *ess1*^{H164R} (this study), *rrp6*Δ (Wyers et al., 2005) and *nab3-11* (Arigo et al., 2006) mutants. As expected, there is some overlap between SAGE transcripts in each mutant background, consistent with a role for each of the three genes, *RRP6*, *NAB3* and *ESS1,* in CUT processing.

F) Supplemental Text and Figures

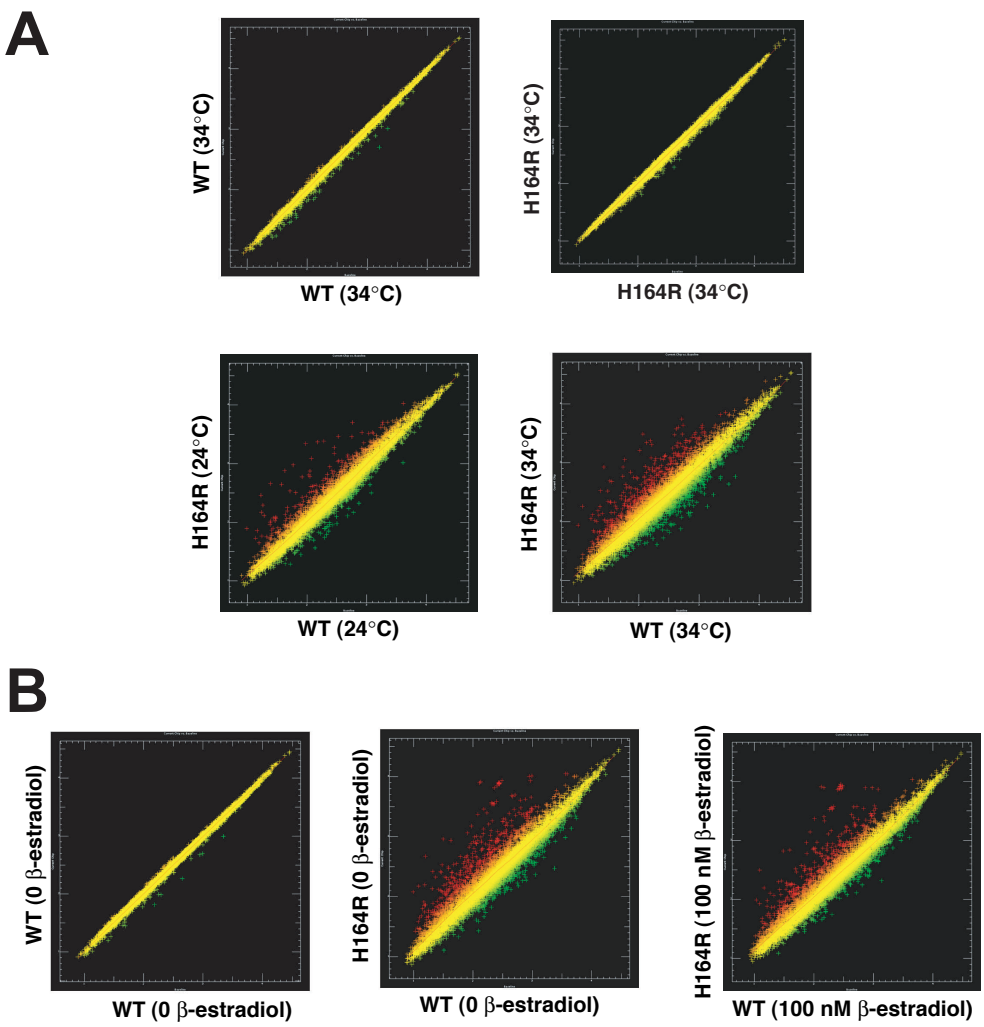

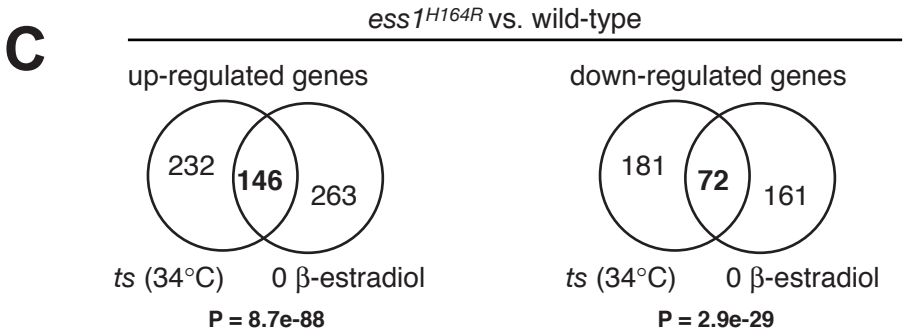

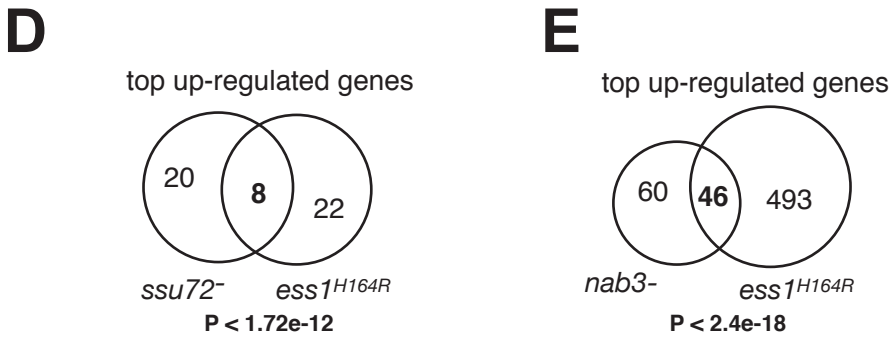

Figure S1

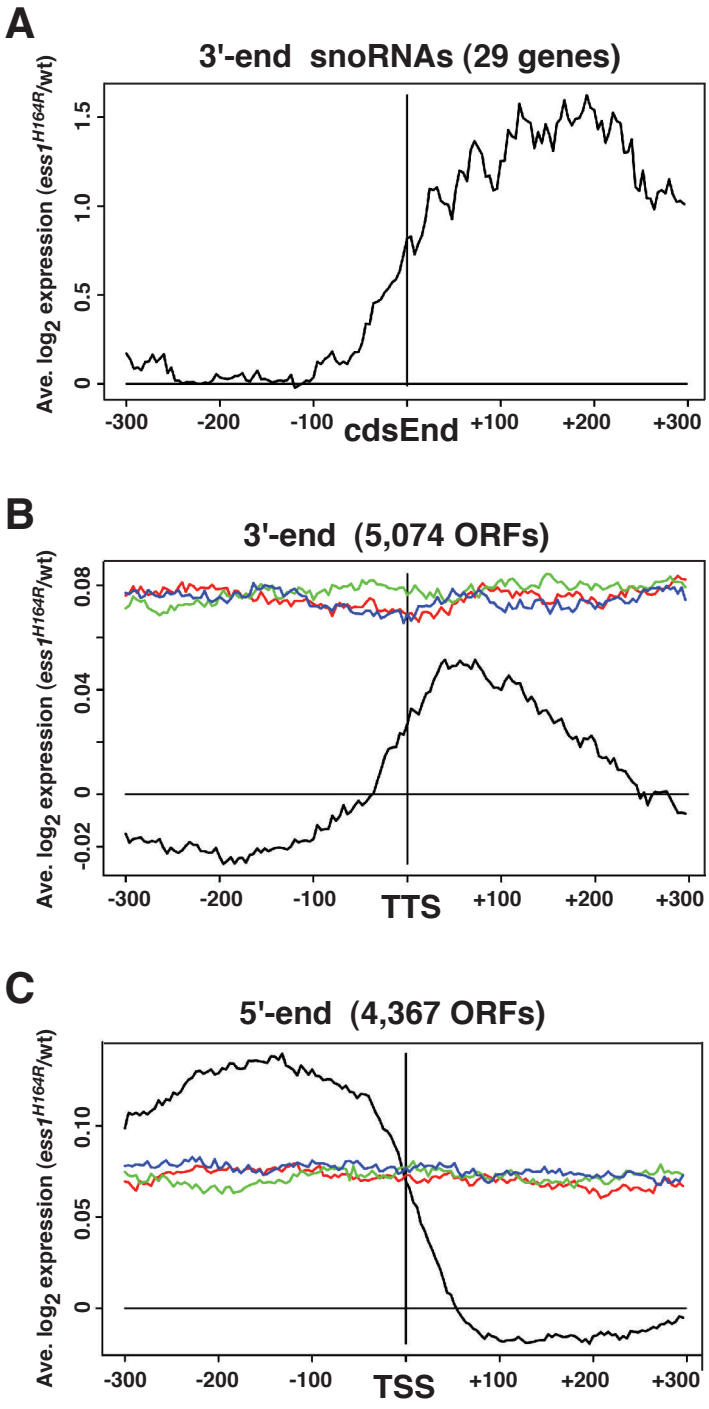
A
3'-end snoRNAs (29 genes)
Ave. log2 expression (ess1H164R/wt)
0
0.5
1.0
1.5
-300
-200
-100
cdsEnd
+100
+200
+300
B
3'-end (5,074 ORFs)
Ave. log2 expression (ess1H164R/wt)
-0.02
0
0.04
0.08
-300
-200
-100
TTS
+100
+200
+300
C
5'-end (4,367 ORFs)
Ave. log2 expression (ess1H164R/wt)
0
0.05
0.10
-300
-200
-100
TSS
+100
+200
+300

Figure S2

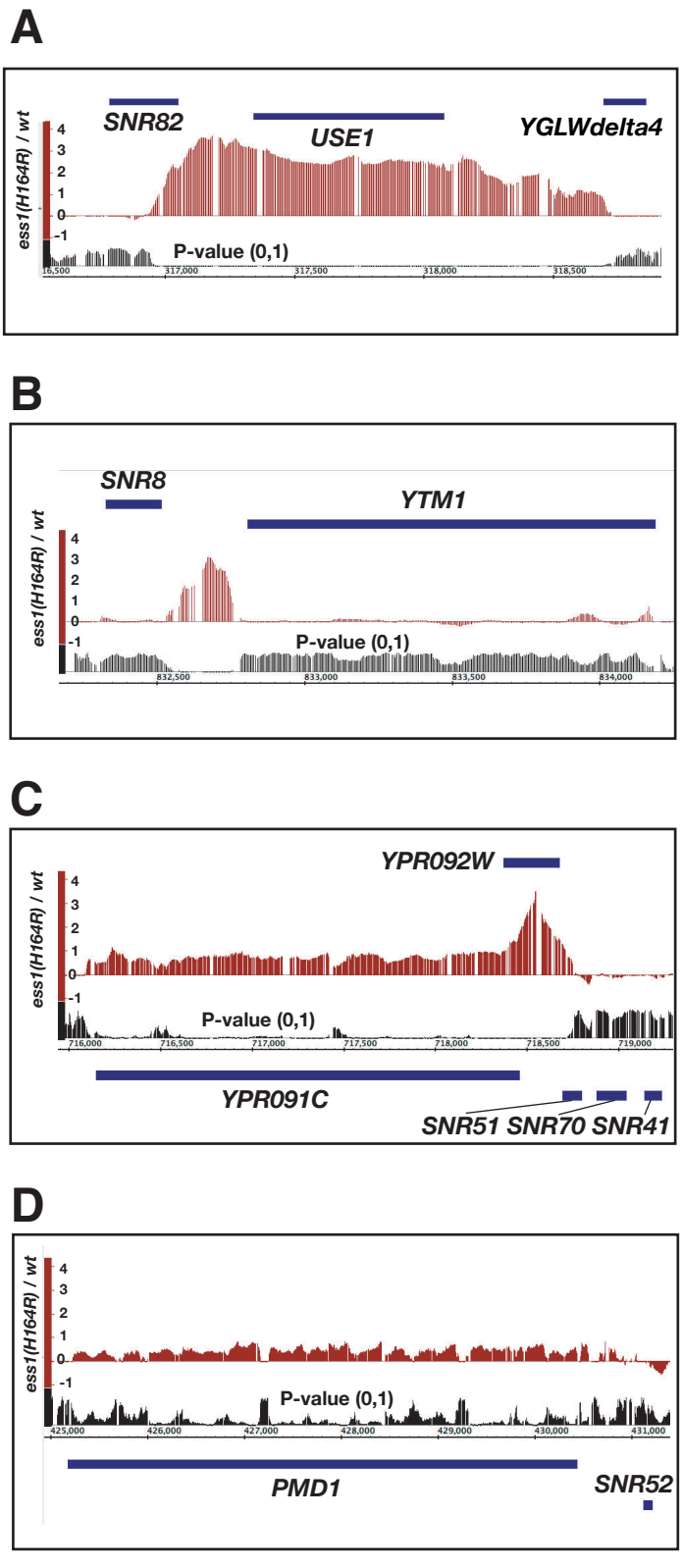
A
SNR82
USE1
YGLWdelta4
ess1(H164R) / wt
4
3
2
1
0
-1
P-value (0,1)
16,500
317,000
317,500
318,000
318,500
B
SNR8
YTM1
ess1(H164R) / wt
P-value (0,1)
832,500
833,000
833,500
834,000
C
YPR092W
ess1(H164R) / wt
P-value (0,1)
716,000
716,500
717,000
717,500
718,000
718,500
719,000
YPR091C
SNR51 SNR70 SNR41
D
ess1(H164R) / wt
P-value (0,1)
425,000
426,000
427,000
428,000
429,000
430,000
431,000
PMD1
SNR52

Figure S3

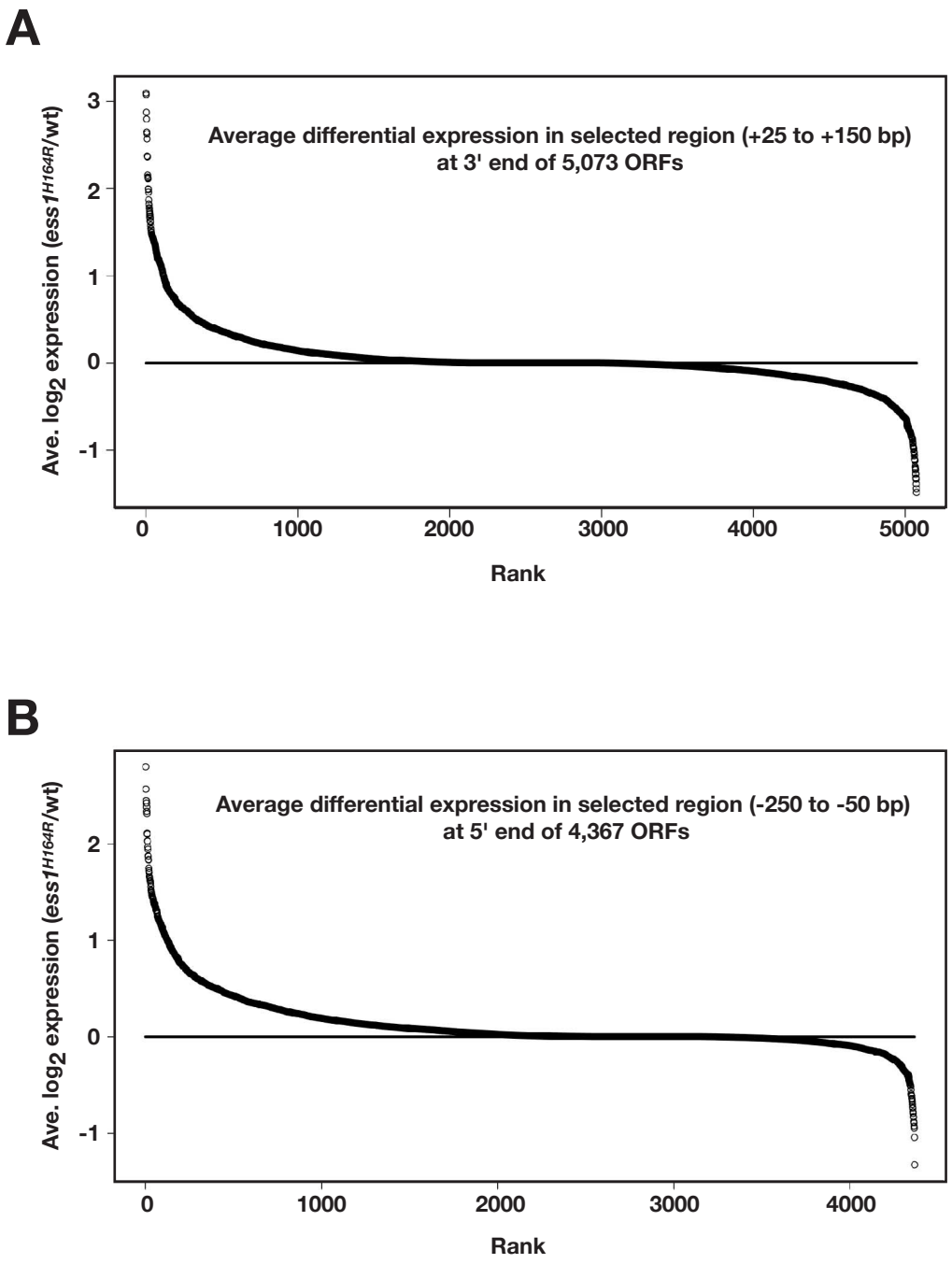
A
Average differential expression in selected region (+25 to +150 bp)
at 3' end of 5,073 ORFs
Ave. log2 expression (ess1H164R/wt)
3
2
1
0
-1
0
1000
2000
3000
4000
5000
Rank
B
Average differential expression in selected region (-250 to -50 bp)
at 5' end of 4,367 ORFs
Ave. log2 expression (ess1H164R/wt)
2
1
0
-1
0
1000
2000
3000
4000
Rank

Figure S4

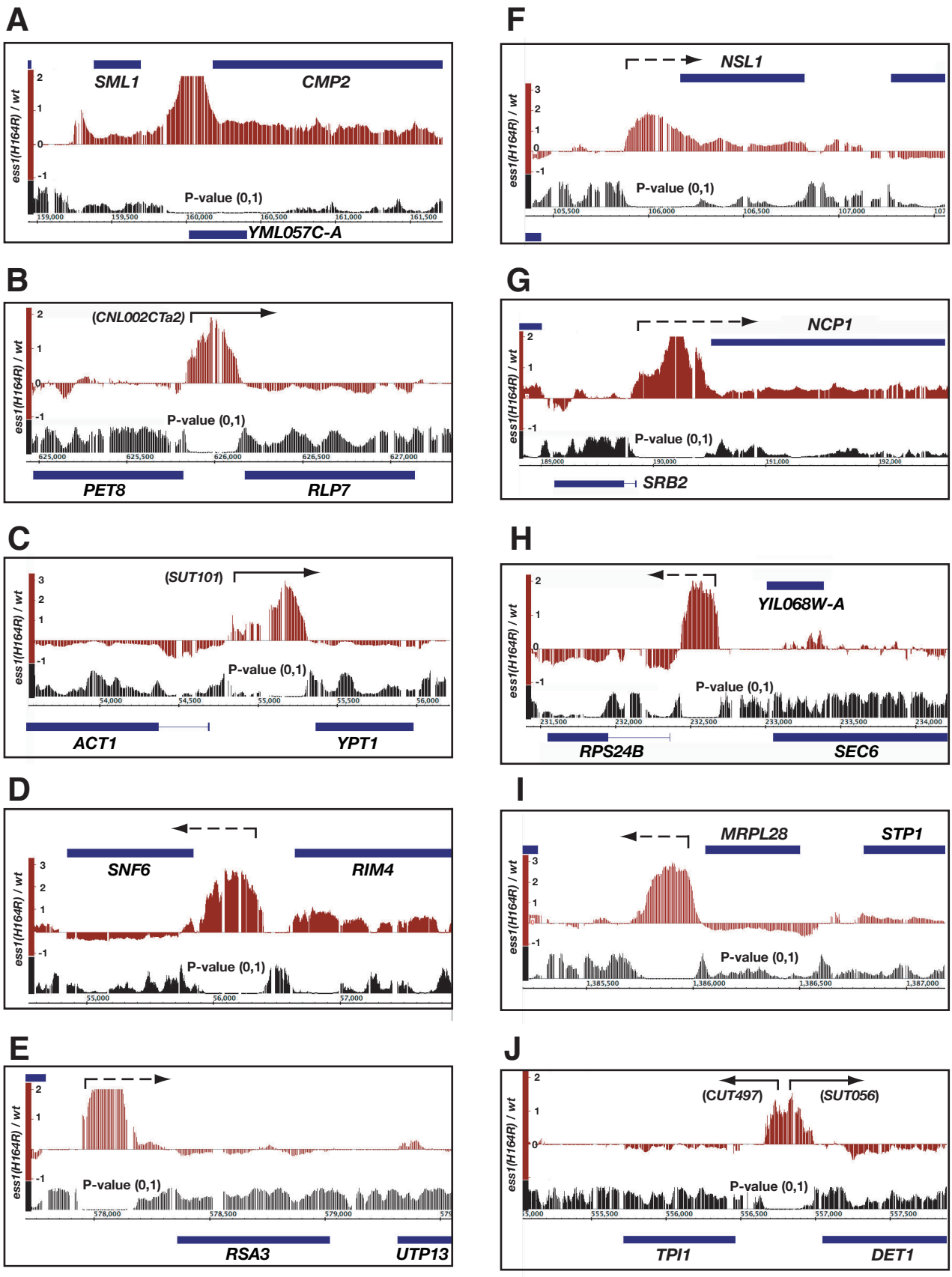
A
SML1
CMP2
ess1(H164R) / wt
P-value (0,1)
YML057C-A
B
(CNL002CTa2)
PET8
RLP7
C
(SUT101)
ACT1
YPT1
D
SNF6
RIM4
E
RSA3
UTP13
F
NSL1
G
NCP1
SRB2
H
YIL068W-A
RPS24B
SEC6
I
MRPL28
STP1
J
(CUT497)
(SUT056)
TPI1
DET1

Figure S5

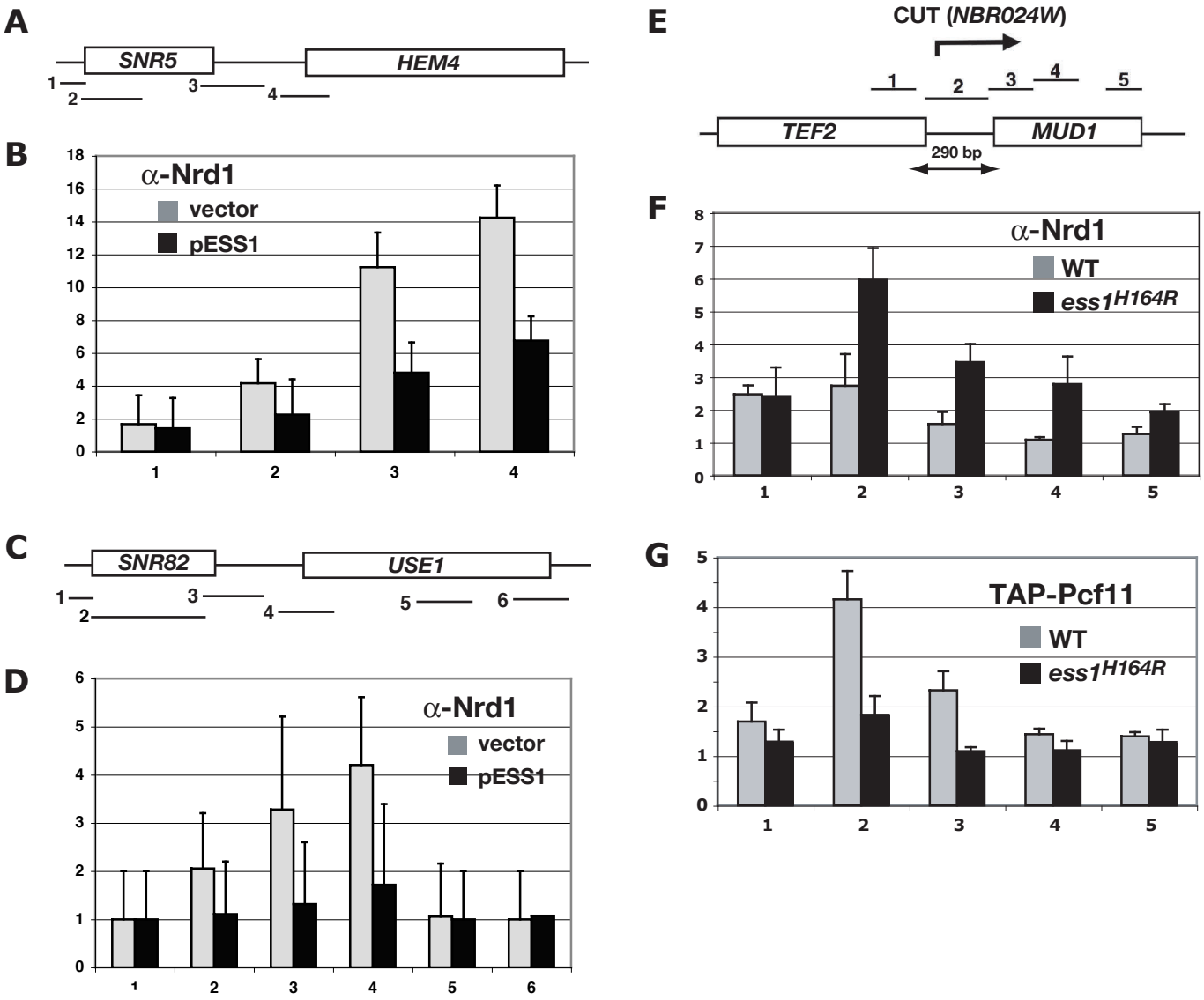
A
SNR5
HEM4
1
2
3
4
B
α-Nrd1
vector
pESS1
C
SNR82
USE1
1
2
3
4
5
6
D
α-Nrd1
vector
pESS1
E
CUT (NBR024W)
1
2
3
4
5
TEF2
MUD1
290 bp
F
α-Nrd1
WT
ess1H164R
G
TAP-Pcf11
WT
ess1H164R

Figure S6

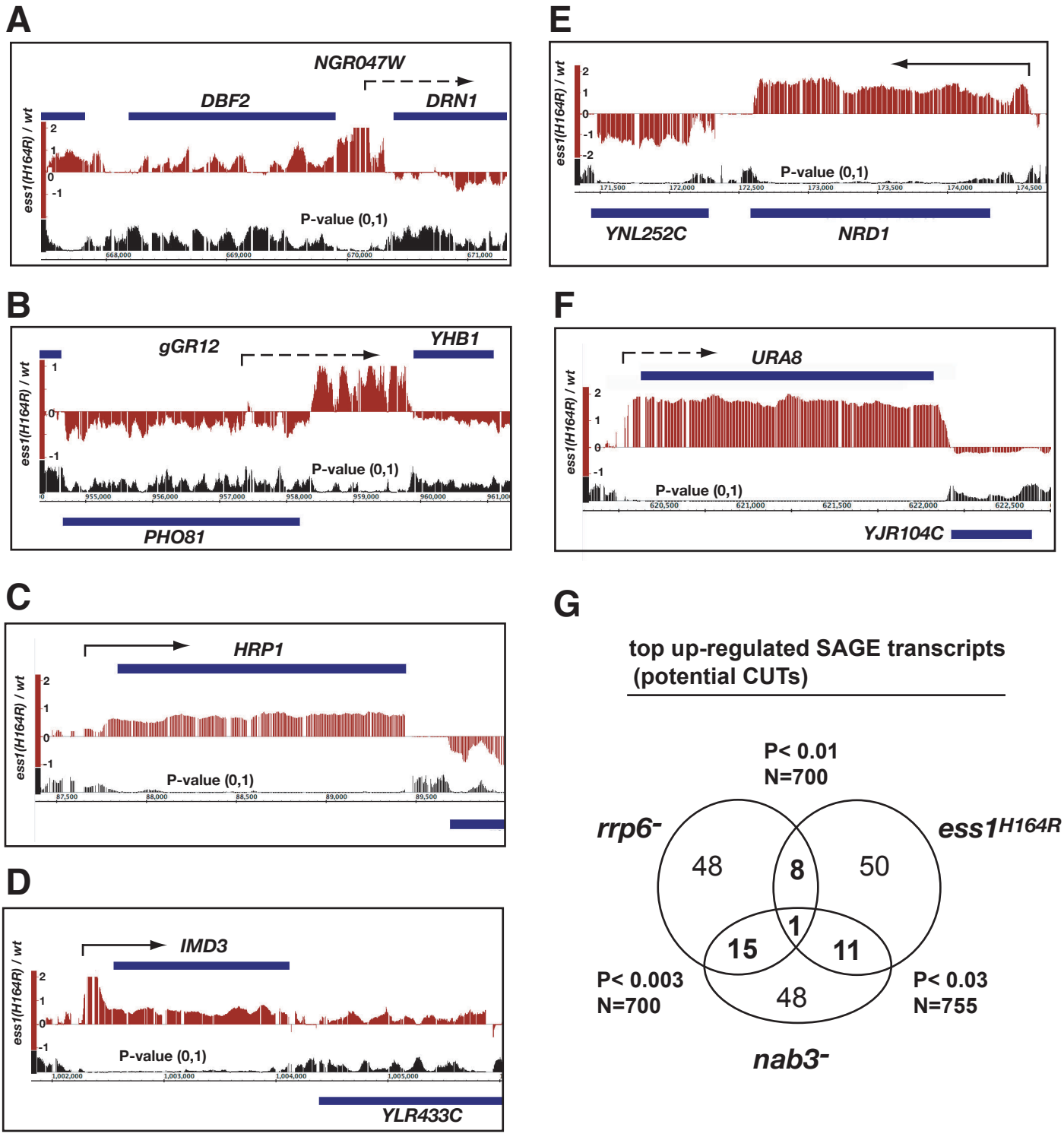
A
NGR047W
DBF2
DRN1
ess1(H164R) / wt
P-value (0,1)
B
gGR12
YHB1
PHO81
C
HRP1
D
IMD3
YLR433C
E
YNL252C
NRD1
F
URA8
YJR104C
G
top up-regulated SAGE transcripts
(potential CUTs)
P< 0.01
N=700
rrp6-
ess1H164R
48
8
50
1
15
11
P< 0.003
N=700
48
P< 0.03
N=755
nab3-

Figure S7

Supplementary Experimental Procedures

Plasmids

Reporter plasmids for snoRNA terminator activity were a gift from Jeff Corden (Carroll et al., 2004) and are derivatives of pRS416 (*CEN, URA3*) that contain an *ADH* promoter, *HIS3* coding region, and *CYC1* terminator. SnoRNA terminator sequences (66bp of *Snr13* or 70bp of *Snr47*) were inserted upstream of the *HIS3* coding region. Three constructs, pAHC-416 (*ADH1-HIS3-CYC1*), pA13HC-416 (*ADH1- Snr13(66)-HIS3-CYC1*) and pA47HC-416 (*ADH-Snr47(70)-HIS3-CYC1*) were transformed in W303-1A, *ess1*^{H164R} (YGD-ts22), 46a and 46a-*nrd1-5* strains to measure the transcription read-through defect. The plasmid pRS424-ESS1 (2µ, *TRP1*) (Ren et al., 2005) was used to overexpress Ess1 in *nrd1-5*, *pcf11-9* and *nab3-11* mutant strains. The plasmids, pRS424-NRD1 (2µ, *TRP1*) (Steinmetz and Brow, 1998), pRS424-PCF11 (2µ, *TRP1*) and pRS424-*NAB3* (2µ, *TRP1*) plasmids were used to overexpress Nrd1, Pcf11 and Nab3, respectively, in W303-1A and *ess1*^{H164R} mutants. Plasmid pRS415-PCF11 (Amrani et al., 1997) was obtained from S. Buratowski (Harvard Med. School), pNAB3.14 (Conrad et al., 2000) from Jeff Corden (Johns Hopkins Univ.) and pRS424 (Christianson et al., 1992) from the laboratory of Phil Heiter (U. British Columbia).

Northern Analysis

For RNA preparations, cells were grown at 30ºC and harvested after a rapid temperature shift to 37ºC (by the addition of prewarmed media) for 0, 30, 60 and 180 minutes. For fractionation, 20-40 µg of total RNA were used per lane. Prehybridization and hybridization was performed at 65°C in a buffer containing 0.5 M Na_2HPO_4, 7% SDS, 1.0mM EDTA and 1% BSA. ^{32}P-labeled probes were prepared from the PCR amplified genomic regions by random priming. Signal was detected using a Molecular Dynamics phosphorimager and ImageQuant software.

Western Analysis

Yeast strains were grown at 30°C with shaking in YEPD or synthetic media lacking the appropriate amino acid to an OD_{600} of 0.6. Cells were collected by centrifugation, washed with ice-cold water and resuspended in 200 ul lysis buffer [200mM Tris –HCl (pH 8.0), 320 mM $(NH_4)_2 SO_4$, 5 mM $MgCl_2$,10 mM EDTA, 10 mM EGTA, 20% glycerol, 1 mM dithiothreitol (DTT), protease and phosphatase inhibitors]. To make the protein extract, the same volume of glass beads was added to the yeast cell suspensions and cell suspensions were vortexed in a cell disruptor for 5 min at 4°C. After centrifugation, the supernatants were kept for immunoblot analysis. Protein concentrations were determined using a BioRad reagent.

Protein extracts (10 ug) were fractionated by SDS-PAGE (8% gels) and transfered to polyvinylidene difluoride membranes (Millipore) for reaction with primary antibodies according to standard procedures. Primary antibodies were H14 (P-Ser5) and 8WG16 (hypophoshorylated-CTD) from Covance, H5 (P-Ser2) from Bethyl, rabbit-anti Ess1 (Wu et al, 2000) and rabbit anti-Nrd1

antibodies (D. Brow). Anti-tubulin antibody (Abcam) was used for a loading control. Secondary monoclonal antibodies (anti-mouse or anti-rabbit immunoglobulin, IgG) conjugated to horseradish peroxidase (Amersham) were used as appropriate. Proteins were visualized using a chemiluminescence reagents (USB).

Quantitative RT-PCR

For quantitative reverse-transcription PCR (Fig. 6A), cells were grown at 25°C and shifted to 34°C for three hours prior to harvesting. RNA was prepared from three independently-grown cultures. RNA preparations were DNaseI treated prior to cDNA synthesis. All PCR primers were tested using standard reactions and examination of the products on ethidium-bromide stained gels. The Comparative C_T method (Applied Biosystems User Manual) was used for quantitation where the amount of target gene amplification is normalized to an *ACT1* internal control. The relative (fold) enrichment is calculated as follows: $2^{-\Delta\Delta C}{}_T = 2^{[\Delta C}{}_T{}^{(control)-\Delta C}{}_T{}^{(expt.)]}$, where $\Delta C_T = C_T$ (sample) - C_T (control). Error bars are standard deviations from the mean log values. Sequences of oligonucleotides used for PCR are given in Table S5.

Chromatin Immunoprecipitation

Chromatin immunoprecipitation was performed essentially as described (Keogh and Buratowski, 2004). 50 ml yeast cultures were grown at 30°C to mid-log phase and fixed with 11% formaldehyde. The crosslinking reaction was stopped by the addition of glycine. Cells were washed and resuspended in FA lysis buffer with protease inhibitors, lysed to isolate chromatin using glass beads (425-600µ). The chromatin was sonicated using a Sonifier 250 (Branson) to an average size of 200-500 bp. Wild-type and *ess1*^{H164R} chromatin was immunoprecipitated using either anti-Rpb3 (1:100 dilution; Neoclone) or anti-Nrd1 (1:100 dilution; gift from D. Brow) antibodies. The immunoprecipitates were incubated with protein G-agarose (for anti-Rpb3) or protein A-agarose (for anti-Nrd1), washed and eluted. TAP-tagged Ess1 immunoprecipitation was performed with anti-protein A, then with protein A-agarose (Sigma). The eluted supernatants and input controls were treated with proteinase K for 1 hr at 42°C and incubated at 65°C for 5 hr to reverse crosslinked protein-DNA complexes. DNA was extracted using phenol/choloroform/isoamylalcohol (25:24:1) and then with chloroform. The DNA was precipitated using 2 vol. EtOH, 1/10 vol. 3M NaOAc and 20 µg glycogen. For each antibody, the immunoprecipitated DNA fragment was isolated from at least three biological replicates. The relative proportion was then analyzed by quantitative real time PCR. For normalization across a set of samples, quantitative real time PCR values (normalized to inputs and a chromosome V control) were summed for each experiment and the sums set to the same arbitrary value for each experiment. The normalized values thus obtained for each ChIP sample were then used to obtain averages and standard deviations (Yu et al., 2006).

Standard Expression Microarray Analysis

Yeast genome YG98S expression arrays (Affymetrix) were used to analyze the expression of WT and mutant strains. Two independent RNA samples were isolated from wild-type (W303-1A) and *ess1*^{H164R} cells after a temperature shift from 30°C to 34°C for 2 hrs. In a second experiment, RNA was prepared from an *ess1*Δ strain expressing wild-type or an H164R mutant allele under control of the *GAL1* promoter. The plasmids used were pRS-315-GAL1p-WT(*ESS1*) and pRS315-GAL1p-H164R (Gemmill et al, 2005), and were under the control of a ß-estradiol-dependent GAL4-ER-VP16 activator (Louvion et al., 1993). At least two independent RNA samples were isolated from cells grown either with ß-estradiol (100nm) or without ß-estradiol (0 hormone) for 90 minutes. Sample preparation and hybridization analysis of the arrays (Affymetrix) were performed according to the manufacturer's guidelines. Hybridization intensity, scatter plots, and change in gene expression of the annotated probesets was analyzed by Microarray Suite 5.0 software and Microsoft Excel. To identify new potential CUTs upregulated in *ess1* mutants, we analyzed the probesets that represent the non-annotated serial analysis of gene expression (SAGE) open reading frames (Velculescu et al., 1997). To compare potential *ess1*-specific CUTs with previously identified CUTs from *rrp6*Δ mutants (Wyers et al., 2005) and *nab3-11 ts*-mutants (Arigo et al., 2006), we used the Affymetrix Yeast S98 array data from http://www.ncbi.nih.gov/geo, accession number GSE2579 and GSE4657, respectively. All resulting analysis included only the probesets that were identified as present by the software. Comparison analysis between *ess1*^{H164R}/WT and *rrp6*Δ/WT and *nab3-11* was performed using Gene Spring (Agilent Technologies) and Microsoft Excel. The SAGE tags located downstream of snoRNAs that overlap with annotated ORFs were excluded from the analysis (Wyers et al., 2005; Table S3).

Tiling Microarray Analysis

RNA was isolated from three biological replicates of wild-type cells and five replicates of *ess1*^{H164R} mutant cells following a shift from 30°C to 34°C for 2 hrs. The RNA from each sample was hybridized to Affymetrix Yeast 1.0 Tiling Array according to the manufacturer's protocols. The data was analyzed using Tiling Analysis Software Version 1.1. The relative $\log_2$ signal intensity files between *ess1*^{H164R} and WT were visualized as graphs using Integrated Genome Browser (IGB) Version 5.12 (http://www.affymetrix.com/support/developer/tools/download_igb.affx).

Bioinformatic Data Analysis

Affymetrix *S. cerevisiae* 1.0R tiling arrays were hybridized and intensities read with Affymetrix AGCC software. .CEL files produced by the AGCC software were analyzed with Affymetrix Tiling Array Software (TAS) v1.1.02. A two-sample TAS analysis was performed with five *ess1*^{H164R} mutant samples as the 'treatment' group and three wild-type control samples as the 'control' group. The resulting .bar file will be available for download at http://www.wadsworth.org/resnres/bios/hanes.htm. Additional TAS analysis specifications were: bandwidth of 50, quantile normalization, probe-level

analysis performed with both perfect match and mismatch probes, signal reported as log2, a conservative selection of a two-sided p-value and BPMAP file Sc03b_MR_v04.bpmap. The 'scale to target intensity' option was not selected. TAS results were output to both .bar files and text files. Visual examination of TAS results was performed using Affymetrix Integrate Genome Browser (IGB) software. PERL scripts were written to read the TAS output text files and perform bioinformatics data analysis. Plots were created in the open source statistics package R.

Gene coordinates in the October 2003 release of the *S. cerevisiae* genome were used with the 1.0R tiling array data along with BPMAP file Sc03b_MR_v04.bpmap (Affymetrix). All ORF and snoRNA coordinates used in analysis were taken from the sgdGene and sgdOther tables, October 2003 release, downloaded from the UCSC Genome Bioinformatics web site.

Investigation revealed a 40 bp offset on chromosome 2 is present with the combination of the 1.0R tiling array chip and BPMAP file Sc03b_MR_v04.bpmap (confirmed by Affymetrix). Further investigation showed offsets on chromosomes 10 and 11. The offset on chromosome 2 is 40 bps and starts at approximately position 97,500 on the chromosome. The offset on chromosome 10 is 219 bp and starts at approximately chromosome position 121,500. The offset on chromosome 11 is more insidious as it gradually increases from 3 to 8 bps from roughly chromosome position 300,000 to the chromosome's end (approximately, position 660,000). For all three chromosomes, the offset is such that the probe is actually the indicated number of bps (40, 219 or 3-8) upstream of the position stated in the signal (and p-value) text files output by TAS. The PERL scripts performed transformations on coordinates of data falling in these known regions of offsets. For chromosome 11, a simplified correction of 6 was used from position 300,000 to the chromosome's end.

Figures S2A, B, C and Supp Figures 7A, B and C all show the **average** differential expression of a 600 bp region centered on the same relative position for a set of ORFs or snoRNAs. The centering point of the plots is coding sequence end (cdsEnd; Fig. S2A), 3' transcription termination site (TTS; Figs. S2B, S7C) or 5' transcription start site (TSS; Figs. S2C, S7A and B).

The particular set of ORFs or snoRNAs to process was determined by examining (Nagalakshmi et al., 2008) Suppl. Tables 4 or 6. ORF coordinates listed in these tables are more recent than the ORF coordinates of the October 2003 release of the *S. cerevisiae* genome (Oct. 2003 coordinates must be used with the 1.0R tiling arrays). The distance to the desired feature (cdsEnd, 5' TSS or 3' TTS, plot specific) was taken from Nagalakshmi et al. (2008) Table S4 or S6 (either "5-UTR_length", "3'-UTR_length", or "uORF_length") and that value was added or subtracted to the Oct 2003 ORF start or end coordinate (taken from sgdGene and sgdOther tables downloaded from the UCSC Bioinformatics web site). This position was then transformed to take into account the offset problems (detailed above). For each ORF (or snoRNA) in the set being processed, this position become the center point from where signal data was extracted.

Differential expression signal data was extracted from the TAS signal output file +/- 300 bps around the center point. Probe spacing in the 1.0R tiling arrays is at best 4 bps and missing probes abound. When extracting the 600 bps of signal data, each of the 600 positions was recorded as

either containing data or not containing data. Once signal data was collected for all ORFs (or snoRNAs) the data was adjusted for strand orientation (all data placed 5' to 3') and centered on each ORF's computed center point (5' TSS, 3' TTS or cdsEnd). The data sets were then collapsed by groups of 4 and each group of 4 averaged over all ORFs in the set. This left 150 total data points – 75 points on either side of the center point (ignoring the fence post issue). The collapsing by 4 addressed the fact that at best, the data would be at 4 bp intervals; if 300 bps of data is desired, the best that can be had with this tiling array is 300 / 4 = 75. However, due to missing probes, each of the 150 generally, had different numbers of positions actually containing data, *i.e.*, the denominator when computing the average signal at each of the 150 positions differs for each position.

The three control lines on Figs S2A, B and C are plots of average differential expression signal data computed on N random draws of 600 bp regions of the tiling array data, where N is the number of ORFs processed in each plot, *i.e.*, 29, 5,074 and 4,367.

ORF or snoRNA gene sets analyzed:

Figure S2A – Average Differential Expression at 3'-end of snoRNAs. From an initial list of 36 snoRNAs, coordinates for 7 snoRNAs were not found in the Oct 2003 UCSC downloaded sgdOther table, leaving data for 29 snoRNA genes.

Figure S2B – Average Differential Expression at 3'-end of ORFs, Genome-wide. Nagalakshmi et al. (2008) Supp. Table 4 contains 5,127 ORFs across chromosomes 1-16 that have a non-zero entry in the "3'-UTR_length" column (mitochondrial ORFs were ignored). 37 ORFs were removed because they are known to be affected by snoRNA read-through; 2 ORFs were removed because they are in the vicinity of where the offset error starts on chromosome 10; 14 ORFs were removed because they were not found in the sgdGene or sgdOther tables, leaving 5,074 genes.

Figure S2C – Average Differential Expression at 5'-end of ORFs, Genome-wide. Nagalakshmi et al. (2008) Supp. Table 4 contains 4,556 ORFs across chromosomes 1-16 that have an entry in the "5'-UTR_length" column (mitochondrial ORFs were ignored). 32 ORFs were removed because they are known to be affected by snoRNA read-through; 2 ORFs were removed because they are in the vicinity of where the offset error starts on chromosome 10; 14 ORFs were removed because they were not found in the sgdGene or sgdOther tables; 141 were removed because they are listed as "Potential_AUG_annotation_error", leaving 4,367 genes.

Suppl. Figs 4A and B. For select regions in Figs. S2B and C, the average differential expression was computed for every ORF in the set. It was necessary to compute an average value, as opposed to computing the total area of the regions, due to missing probes on the chips. Signal data was collected and centered on the 3' TSS and the 5' TTS, and values were rank ordered and plotted. For Suppl. Fig. 4A, the selected region was +25 to +150 relative to the 3' TTS centering point. For Suppl.

Fig. 4B, the average differential expression was computed for each ORF in the region from -250 to -50 relative to the 5' TSS centering point. These regions were chosen because they show the most pronounced differential expression in Figs. S2B and C. The top 100 ORFs from Suppl. Figs. 4A and 4B are listed in Tables S2 and S3.

Supplemental References

Amrani, N., Minet, M., Wyers, F., Dufour, M.E., Aggerbeck, L.P., and Lacroute, F. (1997). PCF11 encodes a third protein component of yeast cleavage and polyadenylation factor I. Mol. Cell. Biol. *17*, 1102-1109.

Arigo, J.T., Eyler, D.E., Carroll, K.L., and Corden, J.L. (2006). Termination of cryptic unstable transcripts is directed by yeast RNA-binding proteins Nrd1 and Nab3. Mol. Cell *23*, 841-851.

Carroll, K.L., Pradhan, D.A., Granek, J.A., Clarke, N.D., and Corden, J.L. (2004). Identification of cis elements directing termination of yeast nonpolyadenylated snoRNA transcripts. Mol. Cell. Biol. *24*, 6241-6252.

Christianson, T.W., Sikorski, R.S., Dante, M., Shero, J.H., and Hieter, P. (1992). Multifunctional yeast high-copy-number shuttle vectors. Gene *110*, 119-122.

Conrad, N.K., Wilson, S.M., Steinmetz, E.J., Patturajan, M., Brow, D.A., Swanson, M.S., and Corden, J.L. (2000). A yeast heterogeneous nuclear ribonucleoprotein complex associated with RNA polymerase II. Genetics *154*, 557-571.

Ganem, C., Devaux, F., Torchet, C., Jacq, C., Quevillon-Cheruel, S., Labesse, G., Facca, C., and Faye, G. (2003). Ssu72 is a phosphatase essential for transcription termination of snoRNAs and specific mRNAs in yeast. EMBO J. *22*, 1588-1598.

Gemmill, T.R., Wu, X., and Hanes, S.D. (2005). Vanishingly low levels of Ess1 prolyl-isomerase activity are sufficient for growth in *Saccharomyces cerevisiae*. J. Biol. Chem. *280*, 15510-15517.

Keogh, M.C., and Buratowski, S. (2004). Using chromatin immunoprecipitation to map cotranscriptional mRNA processing in *Saccharomyces cerevisiae*. Methods Mol. Biol. (Clifton, N.J) *257*, 1-16.

Louvion, J.F., Havaux-Copf, B., and Picard, D. (1993). Fusion of GAL4-VP16 to a steroid-binding domain provides a tool for gratuitous induction of galactose-responsive genes in yeast. Gene *131*, 129-134.

Nagalakshmi, U., Wang, Z., Waern, K., Shou, C., Raha, D., Gerstein, M., and Snyder, M. (2008). The transcriptional landscape of the yeast genome defined by RNA sequencing. Science *320*, 1344-1349.

Nedea, E., He, X., Kim, M., Pootoolal, J., Zhong, G., Canadien, V., Hughes, T., Buratowski, S., Moore, C.L., and Greenblatt, J. (2003). Organization and function of APT, a subcomplex of the yeast cleavage and polyadenylation factor involved in the formation of mRNA and small nucleolar RNA 3'-ends. J. Biol. Chem. *278*, 33000-33010.

Neil, H., Malabat, C., d'Aubenton-Carafa, Y., Xu, Z., Steinmetz, L.M., and Jacquier, A. (2009). Widespread bidirectional promoters are the major source of cryptic transcripts in yeast. Nature *457*, 1038-1042.

Ren, P., Rossettini, A., Chaturvedi, V., and Hanes, S.D. (2005). The Ess1 prolyl isomerase is dispensable for growth but required for virulence in Cryptococcus neoformans. Microbiology *151*, 1593-1605.

Steinmetz, E.J., and Brow, D.A. (1998). Control of pre-mRNA accumulation by the essential yeast protein Nrd1 requires high-affinity transcript binding and a domain implicated in RNA polymerase II association. Proc. Nat. Acad. Sci. USA *95*, 6699-6704.

Thomas, B.J., and Rothstein, R. (1989). Elevated recombination rates in transcriptionally active DNA. Cell *56*, 619-630.

Velculescu, V.E., Zhang, L., Zhou, W., Vogelstein, J., Basrai, M.A., Bassett, D.E., Jr., Hieter, P., Vogelstein, B., and Kinzler, K.W. (1997). Characterization of the yeast transcriptome. Cell *88*, 243-251.

Wu, X., Wilcox, C.B., Devasahayam, G., Hackett, R.L., Arevalo-Rodriguez, M., Cardenas, M.E., Heitman, J., and Hanes, S.D. (2000). The Ess1 prolyl isomerase is linked to chromatin remodeling complexes and the general transcription machinery. EMBO J. *19*, 3727-3738.

Wyers, F., Rougemaille, M., Badis, G., Rousselle, J.C., Dufour, M.E., Boulay, J., Regnault, B., Devaux, F., Namane, A., Seraphin, B.*, et al.* (2005). Cryptic pol II transcripts are degraded by a nuclear quality control pathway involving a new poly(A) polymerase. Cell *121*, 725-737.

Xu, Z., Wei, W., Gagneur, J., Perocchi, F., Clauder-Munster, S., Camblong, J., Guffanti, E., Stutz, F., Huber, W., and Steinmetz, L.M. (2009). Bidirectional promoters generate pervasive transcription in yeast. Nature *457*, 1033-1037.